AD NUMBER
ADB018261
LIMITATION CHANGES

TO:

Approved for public release; distribution is unlimited.

FROM:

Distribution authorized to U.S. Gov't. agencies only; Test and Evaluation; SEP 1976. Other requests shall be referred to Air Force Armament Laboratory, ATTN: DLDL, Eglin AFB, FL 32542.
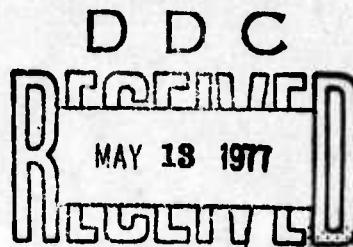
AUTHORITY
ADTC ltr dtd 2 Apr 1980

AFATL-TR-76-109

AEROBALLISTIC RANGE DATA ANALYSIS FOR NONSYMMETRIC CONFIGURATIONS

ARMAMENT SYSTEMS DEPARTMENT

GENERAL ELECTRIC COMPANY

BURLINGTON, VERMONT

SEPTEMBER 1976

FINAL REPORT : MARCH 1976 - SEPTEMBER 1976

D D C

MAY 13 1977

AIR FORCE ARMAMENT LABORATORY

AIR FORCE SYSTEMS COMMAND • UNITED STATES AIR FORCE

EGLIN AIR FORCE BASE, FLORIDA

REPORT DOCUMENTATION PAGE		READ INSTRUCTIONS BEFORE COMPLETING FORM
1. REPORT NUMBER AFATL-TR-76-109	2. GOVT ACCESSION NO.	3. RECIPIENT'S CATALOG NUMBER
4. TITLE (and Subtitle) AEROBALLISTIC RANGE DATA ANALYSIS FOR NONSYMMETRIC CONFIGURATIONS.		5. TYPE OF REPORT & PERIOD COVERED FINAL REPORT - 1 March 1976 to 30 September 1976.
		6. PERFORMING ORG. REPORT NUMBER 76APB551
7. AUTHOR(s) Wayne H. Hathaway Robert H. Whyte		8. CONTRACT OR GRANT NUMBER(s) F08635-76-C-0183
9. PERFORMING ORGANIZATION NAME AND ADDRESS Armament Systems Department General Electric Company Burlington, Vermont		10. PROGRAM ELEMENT, PROJECT, TASK AREA & WORK UNIT NUMBERS Program Element 62602F JON 2547-04-13
11. CONTROLLING OFFICE NAME AND ADDRESS Air Force Armament Laboratory Armament Development and Test Center Eglin Air Force Base, Florida 32542		12. REPORT DATE September 1976
		13. NUMBER OF PAGES 108
14. MONITORING AGENCY NAME & ADDRESS(if different from Controlling Office)		15. SECURITY CLASS. (of this report) UNCLASSIFIED
		15a. DECLASSIFICATION/DOWNGRADING SCHEDULE

16. DISTRIBUTION STATEMENT (of this Report)

Distribution limited to U.S. Government agencies only; this report documents test and evaluation; distribution limitation applied September 1976. Other requests for this document must be referred to the Air Force Armament Laboratory (DLDL), Eglin Air Force Base, Florida 32542

17. DISTRIBUTION STATEMENT (of the abstract entered in Block 20, if different from Report)

19. KEY WORDS (Continue on reverse side if necessary and identify by block number)

AEROBALLISTIC RANGE DATA REDUCTION TECHNIQUE
SPARK RANGE FIRING
FREE FLIGHT DATA ANALYSIS

20. ABSTRACT (Continue on reverse side if necessary and identify by block number)

A model (equations of motion) has been developed which is capable of computing the six-degree-of-freedom trajectory of a nonsymmetric missile. The forces and moments considered to be acting on the missile are described in a body-fixed coordinate system.

The model has been incorporated in a data correlation technique using differential corrections and least-squares theory. A system of five computer programs was developed for complete analysis of ballistic spark range data on a nonsymmetric missile. These are to be used for analysis of data gathered in the USAF Aeroballistic Research Facility located at Eglin AFB.

(Cont)

ABSTRACT (Cont) from page 1473 B)

The model and data correlation technique have been, *(were)* used to analyze ballistic spark range data on two elliptic cones. Individual and simultaneous reductions resulted in probable errors of fit approximately equal to the accuracy of the data. The results of these reductions are presented.
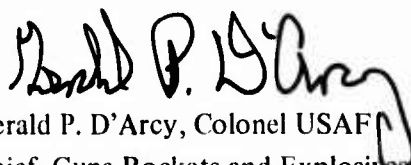
PREFACE

A series of data analysis computer programs was developed during the period from January 1974 to June 1974 by the Armament Systems Department, General Electric Company, Burlington, Vermont, under Contract FO8635-73-C-0165 with the Air Force Armament Laboratory, Eglin Air Force Base, Florida. This report documents the theoretical development and verification of the programs and was prepared by the Armament Systems Department under Contract FO8635-76-C-0183. The program monitor for the Armament Laboratory was Mr. Gerald L. Winchenbach (DLDL).

The principal investigators for the contractor were Wayne H. Hathaway and Robert H. Whyte.

This technical report has been reviewed and is approved for publication.

FOR THE COMMANDER

Gerald P. D'Arcy, Colonel USAF
Chief, Guns Rockets and Explosive Division

ACCESSION for
NTIS   White Section
DDC   Buff Section
UNANNOUNCED
JUSTIFICATION

DISTRIBUTION/AVAILABILITY CODES
AVAIL. and/or SPECIAL

D D C
RECEIVED
MAY 13 1977
D

TABLE OF CONTENTS

SECTION I

INTRODUCTION

Free flight aerodynamic characteristics have been determined by several means of data acquisition. These include the ballistic spark range, wind tunnel, and position radar coupled with a Sonde sun sensor (measures angular orientation relative to the sun, Reference 1). The ballistic spark range has proven to be an accurate means of obtaining aerodynamic characteristics, Reference 2, 3, 4. The dynamic data consists of spark photographs of the model in flight at a specified number of surveyed stations. Each station photographs the model in both the vertical and horizontal planes, thereby allowing for measurement of the six-degree-of-freedom orientation of the model. Dynamic data experimental resolution obtainable from a ballistic spark range is of the order of:

2×10^{-7} seconds in time
0.1 degree in pitch and sideslip angle
1.0 degree in roll angle
0.001 foot in x, y, z coordinates

CORRELATION OF FREE FLIGHT DATA - BACKGROUND

The problems associated with direct correlation of the model (equations of motion) to the test data are threefold, viz. the basic differential equations of motion are nonlinear, the aerodynamic effects are also nonlinear, and the test data are acquired in a coordinate system which is generally not consistent with the model derivation.

The most prevalent method of analyzing ballistic spark range data is based on the linear approximation known as linear theory. Stated briefly, the method uses a linearized model; i.e., a closed form approximate solution to an exact set of differential equations of motion. A least squares fitting technique is used to determine the aerodynamic parameters used in the linearized model. Murphy (Reference 2, 3, 4), MacAllister (Reference 5 and 6), and others at (BRL) Ballistic Research Laboratory as well as Nicolaides (Reference 6-9) and Eikenberry (Reference 10) have developed this method to the extent that certain types of nonlinearities can also be analyzed. However, unless many cycles of data are present and/or multiple experiments conducted, there is only one nonlinear aerodynamic parameter which can be consistently identified, i.e., the static overturning moment.

1

In analyzing free flight data, in 1969 Chapman and Kirk of NASA Ames, California (Reference 11) documented a technique which allows the nonlinear differential equations of motion to be used directly in the data correlation process. The technique eliminates the requirement for closed form approximations to the equations of motion. It is essentially a differential corrections process of forming a system of partial derivatives based on a truncated Taylor's series approximation. The equations of motion and partial derivatives are numerically integrated and solved for the aerodynamic coefficients, based on a least squares formulation, to best fit the data. Independent contributions to this numerical extraction technique were made by Knadler (Reference 12) and Goodman (Reference 13), although the method is usually referred to as the Chapman-Kirk technique. Since this technique includes a very generalized model concept, it is necessary for successful application to have more insight as to which aerodynamic characteristics are pertinent in a given case. The previous limitations caused by nonlinearities in the equations of motion and aerodynamics can be circumvented using this technique.

In late 1969 Whyte and Beliveau (Reference 14-16) documented implementation of the Chapman-Kirk technique for the reduction of experimental ballistic spark range data. Nonlinear aerodynamics were determined from a single data set. Since 1970, the contractor has been very successful in data analysis of a variety of configurations from spark range data, radar data, and Sonde data utilizing this technique (Reference 17-22). A measure of success might be the degrees to which the motion data can be reproduced given the determined aerodynamics and model. The criteria in free flight aerodynamic data analysis should be that the reduction is not successful until the motion data can be reproduced to a probable error equivalent to that of the experimental data.

Until recently, data reduction investigations on free flight aerodynamic data have involved primarily symmetric configurations with the exception of wind tunnel investigations. Interest has been shown in using the ballistic spark range for testing nonsymmetric shapes in free flight (e.g., elliptic cross section re-entry vehicles). Development of a data analysis model and correlation technique capable of handling mass and configuration asymmetries was initiated in January 1974 by the contractor under government contract. Elimination of the assumption of symmetry was complicated by an additional coordinate system transformation and the complexity of the aerodynamics.

SCOPE OF REPORT

The scope can be summarized as follows:

- Model Derivation

- Data Correlation Technique

- Test Case Correlation

The derivation of the model (equations of motion) is done in a coordinate system rigidly attached to the body and rolling with it. With the assumption of symmetry, the model could be defined in a non-rolling coordinate system. Since the dynamic data are acquired in an earth-fixed system, accurate transformations are required to correlate the data with computed values which makes the degrees of freedom highly coupled. Six degrees of freedom are utilized in defining the acceleration and angular momentum equations. The derivation assumes a nonsymmetric configuration. The forces and moments acting on this configuration are defined using aerodynamic coefficients to model the flow phenomenon. Detailed descriptions of the fluid dynamic effects are not discussed. Nonlinearities in the aerodynamics are modeled as polynomial functions of the components of the angle of attack. A thorough understanding of the model derivation is imperative to the overall data analysis technique due to the complexity of the coordinate system transformations and modeling of the flow phenomena. Data analysis using a generalized model containing a large number of aerodynamic coefficients, becomes very abstract without this understanding. Physical significance must be interpreted from the determined aerodynamic coefficients and can only be achieved from the model derivation.

Numerical integration is utilized in correlating the dynamic data to the model. Both the equations of motion and parametric equations are numerically integrated using a fourth order Runge-Kutta Method. As with the case of data analysis of symmetric configurations, the reduction is done in two phases using least-squares theory. The translational motion is reduced first to determine the force coefficients and velocity components required in the reduction of the angular motion. Phase II embodies the angular motion reduction to determine the aerodynamic moment coefficients. Decoupling of the translation and angular motion is required in implementing the Chapman-Kirk technique. Differential corrections using least-squares theory is not amenable to simultaneous correlation of the two motions. This two-phase data analysis concept has been very successful in reducing a large number of data sets on symmetric configurations, Reference 14-22.

Preliminary verification of the model derivation and data correlation technique was done using an ideal test case. Free flight spark range data on the motion of two elliptic bodies with non-equal transverse inertias were then analyzed. The aerodynamic forces and moments on the elliptic bodies were determined with the resulting probable error of fit approximately equivalent to that of the measured data.

3

SECTION II

MODEL DERIVATION

COORDINATE SYSTEM DEFINITIONS

The equations of motion will be derived in a body fixed coordinate system where the x-axis is aligned with the longitudinal axis of the missile, and the coordinate system is free to rotate about that axis at some spin rate, $\dot{\phi}$. In other words, the coordinate system is rigidly attached to the projectile. The inertial frame of reference is the earth. It is assumed that the earth is fixed in space, nonrotating, and flat.

As an additional frame of reference, a fixed plane coordinate system will be defined. This system is similar to the body-fixed coordinate system with the exception that it does not rotate about the missile x-axis, and the y-axis is constrained to be parallel to the XY-plane of the earth fixed coordinate system.

$$i_e, j_e, k_e - \text{Earth Coordinate System}$$
$$i_{mf}, j_{mf}, k_{mf} - \text{Fixed Plane Coordinate System}$$
$$i_m, j_m, k_m - \text{Body-Fixed Coordinate System}$$

To relate the orientation of one coordinate system relative to another, the use of Euler angles (θ_{FP}, ψ_{FP}) will be employed as illustrated in Figure 1, which relates the orientation of fixed plane system to the earth coordinate system. The angles are obtained by rotating a coordinate system, initially coincident with the earth system, about the Z-axis through an angle ψ_{FP} and then about the Y'-axis through the angle θ_{FP}. This results in a y-axis which lies in the XY-plane which is part of the definition of the fixed plane coordinate system. To extend this to the body-fixed system, a rotation about the x-axis is required as illustrated in Figure 2. The definition of the missile velocity vector components is also indicated.

EQUATIONS OF MOTION

The aerodynamic forces and moments are to be defined in the body-fixed coordinate system. Therefore, the equations of motion must be derived based on the acceleration and angular momentum defined in the body-fixed system relative to the inertial frame of reference. Beginning with Newton's second Law, the acceleration and angular momentum will be defined in the body-fixed coordinate system, where the center of gravity of the projectile need not be on the x-axis.

4

Figure 1. Fixed Plane Coordinate System
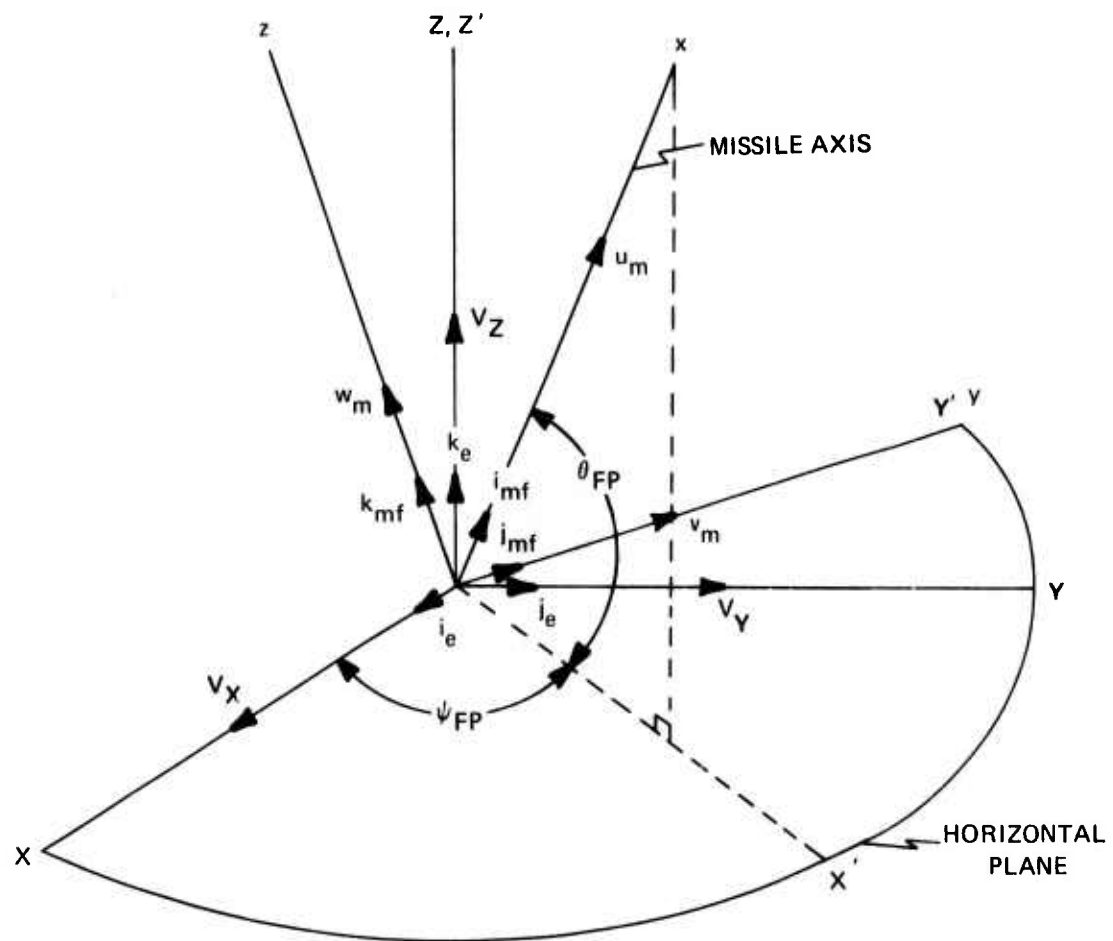
X, Y, Z – Earth-Fixed Coordinates

X', Y', Z' – Intermediate Coordinate System (after first rotation – ψ)

x, y, z – Fixed Plane Coordinate System
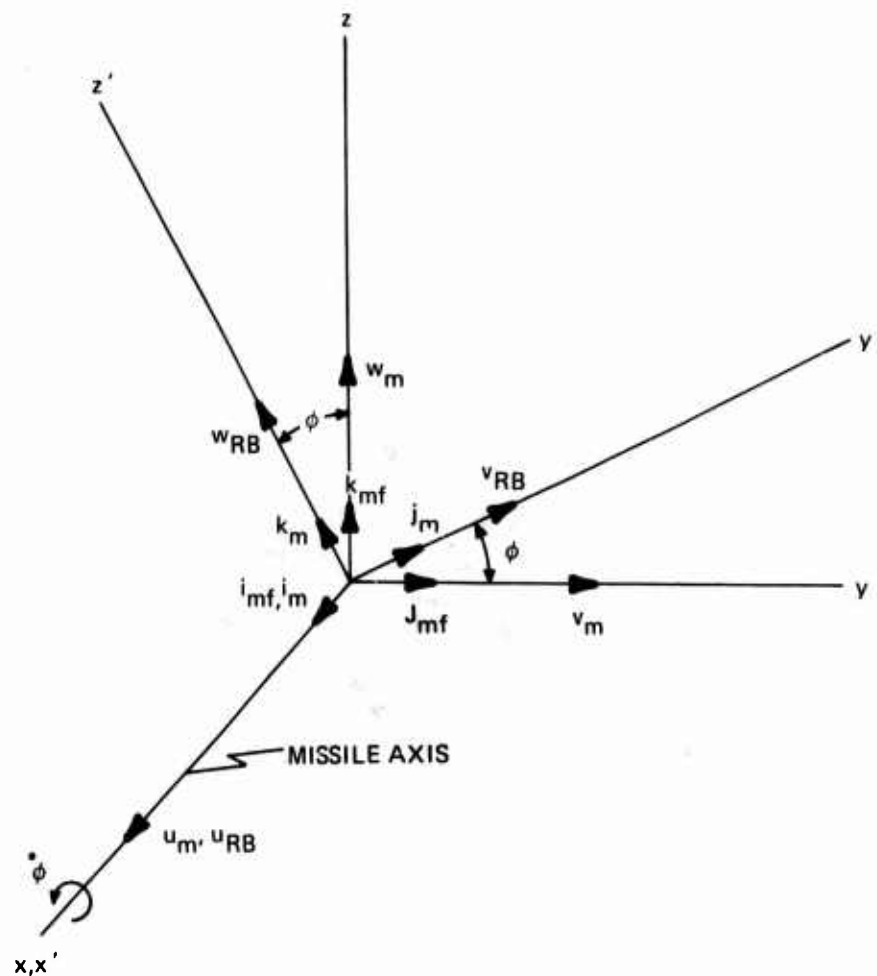
x, y, z — Fixed Plane Coordinate System

x′, y′, z′ — Body-Fixed Coordinate System

Figure 2. Body-Fixed Coordinate System

6

$$\vec{F} = m\left[\frac{d_m \vec{V}}{dt} + \vec{\omega}_T \times \vec{V}\right] \tag{1}$$

$$\vec{L} = \frac{d_m \vec{J}}{dt} + \vec{\omega}_T \times \vec{J} \tag{2}$$

where:

$$\vec{V} = u_{RB}\vec{i}_m + v_{RB}\vec{j}_m + w_{RB}\vec{k}_m \tag{3}$$

$$\vec{\omega}_T = p\vec{i}_m + q\vec{j}_m + r\vec{k}_m \tag{4}$$

$$\vec{J} = [\,I\,]\,\vec{\omega}_T \tag{5}$$

[I] is the mass moment of inertia tensor.

The moment of inertia tensor will be defined such that the body fixed x'y'- plane is a plane of mirror symmetry (i.e. $I_{xz} = I_{yz} = 0$).

Equations (1) through (5) will be stated in terms of the body-fixed components. The following equations of motion are obtained after the vector multiplications and cross products.

$$[\,I\,] = \begin{bmatrix} I_x & -I_{xy} & 0 \\ -I_{xy} & I_y & 0 \\ -0 & 0 & I_z \end{bmatrix} \tag{6}$$

$$F_x = m(\dot{u}_{RB} + qw_{RB} - rv_{RB}) \tag{7a}$$

$$F_y = m(\dot{v}_{RB} + ru_{RB} - pw_{RB}) \tag{7b}$$

$$F_z = m(\dot{w}_{RB} + pv_{RB} - qu_{RB}) \tag{7c}$$

$$L_p = I_x \dot{p} - I_{xy} \dot{q} + I_z qr + I_{xy} rp - I_y qr \tag{8a}$$

$$L_q = I_y \dot{q} - I_{xy} \dot{p} + I_x pr - I_{xy} qr - I_z pr \tag{8b}$$

$$L_r = I_z \dot{r} - I_{xy} p^2 + I_y pq - I_x pq + I_{xy} q^2 \tag{8c}$$

The equations of motion are desired in the form of linear and angular acceleration (body fixed) as a function of the aerodynamic forces and moments. Simultaneous solution of Equations (8a) and (8b) and rearrangement of the remaining Equations (7) and (8) equations will result in the desired form.

$$\dot{u}_{RB} = r\,v_{RB} - q w_{RB} + F_x/m \tag{9a}$$

$$\dot{v}_{RB} = p w_{RB} - r u_{RB} + F_y/m \tag{9b}$$

$$\dot{w}_{RB} = q u_{RB} - p v_{RB} + F_z/m \tag{9c}$$

$$\dot{p} = \frac{I_y L_p + I_{xy} L_q - (I_x + I_y - I_z) I_{xy}\, pr + (I_{xy}^2 + I_y (I_y - I_z))\, qr}{(I_x I_y - I_{xy}^2)} \tag{10a}$$

$$\dot{q} = \frac{I_x \dot{L}_q + I_{xy} L_p + (I_x + I_y - I_z) I_{xy}\, qr + (I_x (I_z - I_x) - I_{xy}^2)\, pr}{(I_x I_y - I_{xy}^2)} \tag{10b}$$

$$\dot{r} = \frac{L_r + I_{xy} (p^2 - q^2) + (I_x - I_y)\, pq}{I_z} \tag{10c}$$

Equations (9) and (10) represent the six-degree-of-freedom differential equations of motion derived in the body-fixed coordinate system. Once the definition of the forces and moments is made, the solution to these equations will define the six-degree-of-freedom free flight motion of a nonsymmetric missile in body-fixed coordinates. The equations of motion have been derived in the body-fixed coordinate system for the purpose of defining the forces and moments. Their solution results in the translational and angular motion of the missile relative to the body-fixed coordinate system. An additional set of transformation differential equations will be used for defining the motion relative to the earth. The data acquired from a ballistic spark range is in terms of this motion. Therefore, the transformation equations are necessary for correlation of the equations of motion to the data. These transformation equations are expressed in terms of the body-fixed velocity components (u_{RB}, v_{RB}, p, q, and r), the fixed plane Euler angles (θ_{FP}, ψ_{FP}), and the angle of rotation about the missile axis (ϕ).

$$V_X = u_{RB}\, COS\theta_{FP}\, COS\psi_{FP} + v_{RB}\, (SIN\theta_{FP} SIN\phi COS\psi_{FP} - COS\phi SIN\psi_{FP})$$
$$+ w_{RB}\, (SIN\theta_{FP} COS\phi COS\psi_{FP} + SIN\phi SIN\psi_{FP}) \tag{11a}$$

$$V_Y = u_{RB} COS\theta_{FP} SIN\psi_{FP} + v_{RB}\, (SIN\theta_{FP} SIN\phi SIN\psi_{FP} + COS\psi_{FP} COS\phi)$$
$$+ w_{RB}\, (SIN\theta_{FP} COS\phi SIN\psi_{FP} - COS\psi_{FP} SIN\phi) \tag{11b}$$

$$V_Z = u_{RB} SIN\theta_{FP} + v_{RB} SIN\phi COS\theta_{FP} + w_{RB} COS\phi COS\theta_{FP} \tag{11c}$$

$$\dot{\phi} = p + \text{TAN}\,\theta_{+p}\,[\,q\,\text{SIN}\phi + r\,\text{COS}\psi\,] \tag{11d}$$

$$\dot{\theta} = q\,\text{COS}\phi - r\,\text{SIN}\phi \tag{11e}$$

$$\dot{\psi} = [\,q\,\text{SIN}\phi + r\,\text{COS}\phi\,]\,/\,\text{COS}\theta_{+p} \tag{11f}$$

AERODYNAMIC FORCES AND MOMENTS

The forces and moments resulting from fluid flow phenomena on a missy be defined in coefficient form as is done in classical aerodynamics, Re definitions of the aerodynamics are based on Reference 23. Depending on the properties and complexity of the missile configuration, these forces and moments could be nonlinear functions of the total angle of attack ($\overline{a}$) or components of the angle of attack (a, β). The angles $\overline{a}$, a, and β are defined in Figure 3. In a ballistic range the Mach number change during the flight is relatively small. Mach number effects will therefore be neglected, with the exception of the axial force, in this derivation since the application of the final equations of motion is to analyze free flight motion in a ballistic range. The nonlinearities with angle of attack will be modeled as polynomial functions of the sine of the total angle of attack or its components. Experience has shown this method of modeling to be adequate (Reference 14-22).

BASIC FORCES AND MOMENTS

The primary aerodynamic forces and moments acting on a body in free flight are illustrated in Figure 3. The forces are a result of drag, lift, and pressure distribution around a rotating body, while the moments are a result of skin friction and the fact that the forces act at the center of pressure which is not coincident with the center of gravity. A more detailed description of these primary forces and moments is as follows:

C_x - Axial Force

  - Acts along the body axis opposite to the u_{RB} velocity vector

C_z - Normal Force (a)

  - Acts in the a-pitch plane perpendicular to the body axis

C_y - Normal Force (β)

  - Acts in the β-sideslip plane perpendicular to the body axis

C_{zp} - Magnus Force (β)

  - Acts perpendicular to the β-sideslip plane

9
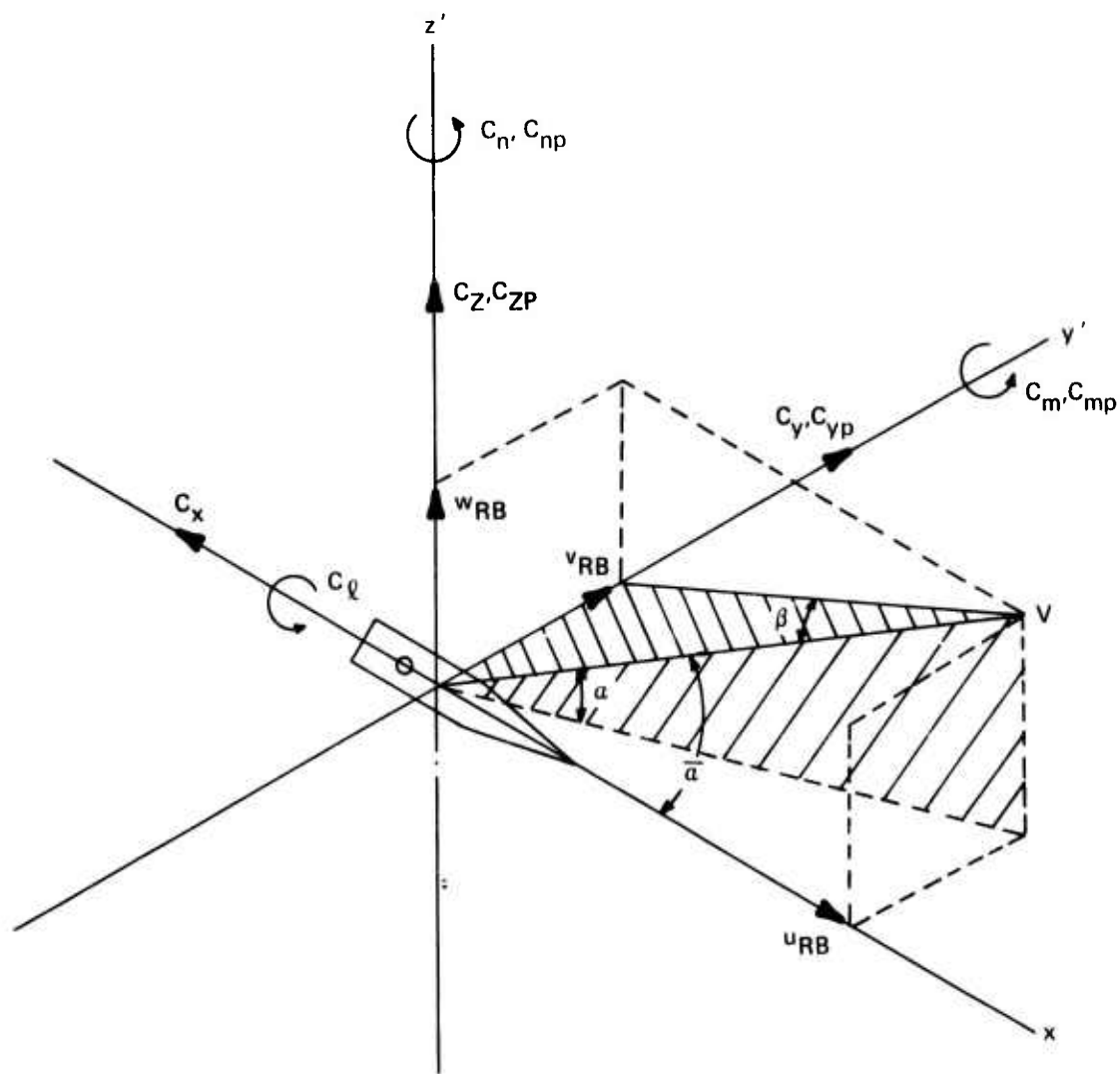
Figure 3. Body-Fixed Coordinate System with Basic Force and Moment Definition

C_{yp} - Magnus Force (a)

- Acts perpendicular to the a-pitch plane

C_ℓ - Roll moment
- Acts about x'-axis

C_m - Pitching Moment (a)

- Acts about y'-axis

C_n - Pitching Moment (β)

- Acts about $-$ z'-axis

C_{mp} - Magnus Moment (β)

- Acts about y'-axis

C_{np} - Magnus Moment (a)

- Acts about z'-axis

The magnus and spin forces and moments are dependent on the nondimensional spin parameter, pd/2v, since they are only associated with flow phenomena about a spinning body. The forces and moments will be modeled as coefficient derivative functions of the sine of the components of the total angle of attack, $\overline{a}$.

$$SIN\ a = \frac{^wRB}{V} \tag{12a}$$

$$SIN\ \beta = \frac{^vRB}{V} \tag{12b}$$

Therefore:

$$C_x = \overline{q}\ A\ (\ C_{xo} + C_{xa2}\ (\frac{^wRB}{V})^2 + C_{x\beta2}\ (\frac{^vRB}{V})^2 + C_{xM}\ (M - MREF)\ ) \tag{13a}$$

$$C_z = \overline{q}\ A\ (\ C_{za}\ (\frac{^wRB}{V}) + C_{za3}\ (\frac{^wRB}{V})^3\ ) \tag{13b}$$

11

$$C_y = \bar{q} A \left(C_{y\beta} \left(\frac{^vRB}{V}\right) + C_{y\beta 3} \left(\frac{^vRB}{V}\right)^3 \right) \tag{13c}$$

$$C_{zp} = \bar{q} A \left(C_{zp\beta} \left(\frac{pd}{2V}\right)\left(\frac{^vRB}{V}\right) \right) \tag{13d}$$

$$C_{yp} = \bar{q} A \left(C_{ypa} \left(\frac{pd}{2V}\right)\left(\frac{^wRB}{V}\right) \right) \tag{13e}$$

$$C_\ell = \bar{q} Ad \left(C_{\ell p} \left(\frac{pd}{2V}\right) \right) \tag{13f}$$

$$C_m = \bar{q} Ad \left(C_{ma} \left(\frac{^wRB}{V}\right) + C_{ma3} \left(\frac{^wRB}{V}\right)^3 \right) \tag{13g}$$

$$C_n = \bar{q} Ad \left(C_{n\beta} \left(\frac{^vRB}{V}\right) + C_{n\beta 3} \left(\frac{^vRB}{V}\right)^3 \right) \tag{13h}$$

$$C_{mp} = \bar{q} Ad \left(C_{mp\beta} \left(\frac{pd}{2V}\right)\left(\frac{^vRB}{V}\right) \right) \tag{13i}$$

$$C_{np} = \bar{q} Ad \left(C_{npa} \left(\frac{pd}{2V}\right)\left(\frac{^wRB}{V}\right) \right) \tag{13j}$$

DAMPING MOMENT

The yaw damping moment being considered is defined as acting perpendicular to the body axis but independent of the yaw (angle of attack) plane orientation. It is dependent on the angular velocity components, q and r. Modeling of the damping moment is accomplished using the aerodynamic coefficients C_{mq} and C_{nr}. The sense of these components is depicted in Figure 4.

$$\bar{C}_{mq} = \bar{q} Ad \left(\frac{qd}{2V}\right) \left(C_{mq} + C_{mq2} \left(\frac{^wRB}{V}\right)^2 \right) \tag{14a}$$

$$\bar{C}_{nr} = \bar{q} Ad \left(\frac{rd}{2V}\right) \left(C_{nr} + C_{nr2} \left(\frac{^vRB}{V}\right)^2 \right) \tag{14b}$$

It should be noted that a more exact definition of the damping moment would be to consider it as being dependent on the cross-angular velocity components q' and r' which are coincident with, and normal to, the angle of attack plane, respectively (Reference 23). These components are shown in Figure 4. The more exact definition would introduce cross-damping terms into the equations of motion.

Figure 4. Damping Moment and Body-Fixed Force-Moment Definition

BODY-FIXED ASYMMETRIES

Body-fixed aerodynamic forces and moments are due to misalignment, cant, or asymmetry of body and/or lifting surfaces. Figure 4 depicts a center of gravity which is completely nonplanar relative to the primary body axes (x'-y'-z'). These forces and moments are commonly referred to as trims. The existence of trims would cause the free flight angular motion of a body to oscillate about an axis which is not coincident with the initial body x'-axis. The body fixed forces and moments will be defined by the aerodynamic coefficients C_{yo}, C_{no}, C_{zo}, and C_{mo} as illustrated in Figure 4. The forces C_{yo} and C_{zo} act at the center of pressure causing the moments C_{no} and C_{mo} about the center of gravity, respectively. Trims along and about the body X'-axis are absorbed in the axial force and roll moment coefficients as defined in Equations (13a and f).

AERODYNAMIC EFFECT DUE TO CROSS FLOW ORIENTATION

These effects are due to the orientation of the aerodynamic surfaces with respect to the cross flow. The orientation of these surfaces will be defined by the aerodynamic roll angle, ϕ', which is the clockwise rotation by the aerodynamic surfaces with respect to the cross flow as illustrated in Figure 5. The cross flow velocity vector is the resultant velocity perpendicular to the primary body axis, x'.

$$\phi' = TAN^{-1}\left[\frac{v_{RB}}{w_{RB}}\right] - \zeta \tag{15}$$

The phase angle, ζ, due to the initial orientation of the plane of symmetry relative to the body-fixed coordinate system axes should typically be zero. The most significant induced aerodynamic effects resulting from missile orientation relative to cross flow are generally the induced rolling moment, the induced side force, and the induced side moment (Reference 23). Since the cross flow will have some effect on normal force and pitching moment, they will be considered also. These forces and moments are a function of the total angle of attack in addition to the aerodynamic roll angle.

$$C_{y\phi a} SIN^2 \bar{a} SIN (n\phi') \qquad = \text{ Induced side force acts} \atop \text{perpendicular to yaw plane} \tag{16a}$$

$$C_{n\phi a} SIN^2 \bar{a} SIN (n\phi') \qquad = \text{ Induced side moment} \tag{16b}$$

$$C_{N\phi a} SIN^2 \bar{a} SIN (n\phi') \qquad = \text{ Induced normal force acts in} \atop \text{yaw plane} \tag{16c}$$

$$C_{m\phi a} SIN^2 \bar{a} SIN (n\phi') \qquad = \text{ Induced pitching moment} \tag{16d}$$

14
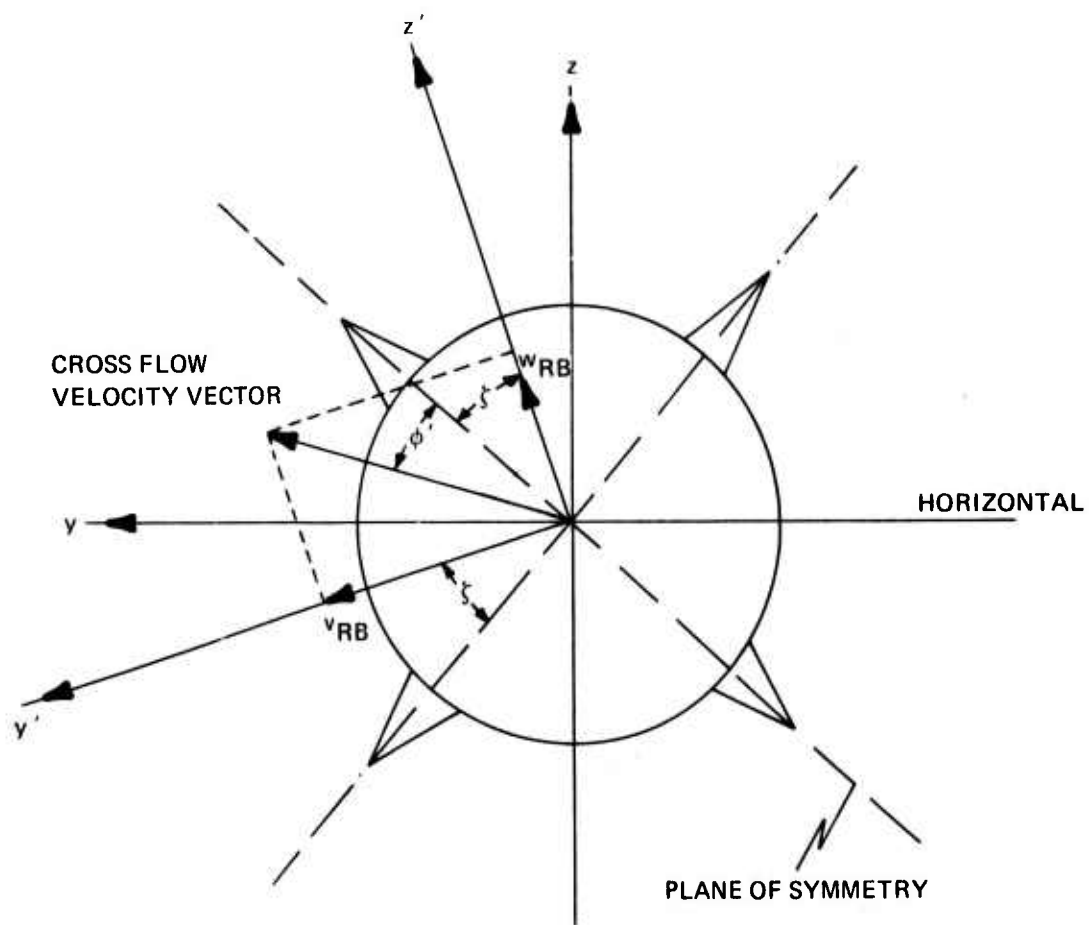
Figure 5. Aerodynamic Surfaces Relative to Cross Flow

15

$$C_{\ell\phi a}\text{SIN}^2\,\bar{a}\,\text{SIN}\,(\,n\phi'\,) \quad = \text{Induced rolling moment} \tag{16e}$$

$$n = \text{number of axially symmetric fins or surfaces}$$

GRAVITATIONAL FORCE

The force of gravity will be defined in vector notation as follows:

$$\text{Gravity Force} = -\,mg\,\vec{k}_e \tag{17}$$

Replacing the unit vector $\vec{k}_e$ by its representation in the body fixed coordinate system, the gravity force will be resolved into components which are consistent with the definition of the aerodynamic forces.

$$-mg\vec{k}_e = mg\text{SIN}\theta_{FP}\vec{i}_m - mg\text{COS}\theta_{FP}\text{SIN}\phi\vec{j}_m - mg\text{COS}\theta_{FP}\text{COS}\phi\vec{k}_m \tag{18}$$

It is assumed that the earth is flat, and the earth's rotation may be neglected.

SUMMARY OF FORCES AND MOMENTS

Combining the forces and moments which have been defined in Equations (12) through (18), the terms F_x, F_y, F_z, L_p, L_q, L_r will be defined for substitution into Equations (9) and (10).

$$F_x = \bar{q}A\left[\,C_{xo} + C_{xa2}\left(\frac{w_{RB}}{V}\right)^2 + C_{x\beta2}\left(\frac{v_{RB}}{V}\right)^2 + C_{xM}\,(M - MREF)\,\right] + mg\text{SIN}\theta_{FP} \tag{19}$$

$$
\begin{aligned}
F_y = \bar{q}A\,\Big[\,&C_{yo} + C_{y\beta}\left(\frac{v_{RB}}{V}\right) + C_{y\beta3}\left(\frac{v_{RB}}{V}\right)^3 + C_{ypa}\left(\frac{pd}{2V}\right)\left(\frac{w_{RB}}{V}\right) \\
&-C_{N\phi a}\text{SIN}^2\bar{a}\,\text{SIN}(n\phi')\left(\frac{v_{RB}}{V}\right) + C_{y\phi a}\text{SIN}^2\bar{a}\,\text{SIN}(n\phi')\left(\frac{w_{RB}}{V}\right)\,\Big] \\
&- mg\text{COS}\theta_{FP}\text{SIN}\phi
\end{aligned} \tag{20}
$$

$$
\begin{aligned}
F_z = \bar{q}A\,\Big[\,&C_{zo} + C_{za}\left(\frac{w_{RB}}{V}\right) + C_{za3}\left(\frac{w_{RB}}{V}\right)^3 + C_{zp\beta}\left(\frac{pd}{2V}\right)\left(\frac{v_{RB}}{V}\right) \\
&-C_{N\phi a}\text{SIN}^2\bar{a}\,\text{SIN}(n\phi')\left(\frac{w_{RB}}{V}\right) - C_{y\phi a}\text{SIN}^2\bar{a}\,\text{SIN}(n\phi')\left(\frac{v_{RB}}{V}\right)\,\Big] \\
&- mg\text{COS}\theta_{FP}\text{COS}\phi
\end{aligned} \tag{21}
$$

16

$$L_p = \overline{q}Ad \left[C_{\ell p}\left(\frac{pd}{2V}\right) + C_{\ell \phi a}SIN^2\,\overline{a}\,SIN(n\phi') \right. \tag{22}$$

$$L_q = \overline{q}Ad \left[C_{mo} + C_{ma}\left(\frac{w_{RB}}{V}\right) + C_{ma3}\left(\frac{w_{RB}}{V}\right)^3 + \left(\frac{qd}{2V}\right)\left(C_{mq} + C_{mq2}\left(\frac{w_{RB}}{V}\right)^2 \right) \right. \tag{23}$$

$$+ C_{mp\beta}\left(\frac{pd}{2V}\right)\left(\frac{v_{RB}}{V}\right) + C_{m\phi a}SIN^2\,\overline{a}\,SIN(n\phi')\left(\frac{w_{RB}}{V}\right)$$

$$+ C_{n\phi a}SIN^2\,\overline{a}\,SIN(n\phi')\left(\frac{v_{RB}}{V}\right) \right]$$

$$L_r = \overline{q}Ad \left[C_{no} + C_{n\beta}\left(\frac{v_{RB}}{V}\right) + C_{n\beta3}\left(\frac{v_{RB}}{V}\right)^3 + \left(\frac{rd}{2V}\right)\left(C_{nr} + C_{nr2}\left(\frac{v_{RB}}{V}\right)^2\right) \right. \tag{24}$$

$$+ C_{npa}\left(\frac{pd}{2V}\right)\left(\frac{w_{RB}}{V}\right) - C_{m\phi a}SIN^2\,\overline{a}\,SIN(n\phi')\left(\frac{v_{RB}}{V}\right)$$

$$+ C_{n\phi a}SIN^2\,\overline{a}\,SIN(n\phi')\left(\frac{w_{RB}}{V}\right) \right]$$

DATA CORRELATION TECHNIQUE

DIFFERENTIAL CORRECTIONS (SENSITIVITY EQUATIONS)

The essential steps of the analysis are briefly summarized. The exact equations of motion are derived containing all necessary aerodynamic coefficients. By integration of the equations of motion the theoretical trajectory is obtained. The actual trajectory is known from the ballistic range test data. The gist of the method is to adjust the aerodynamic coefficients contained in the equations of motion in such a way that the generated trajectory matches the actual. The mathematical treatment is a sensitivity analysis. The sensitivity equations or parametric differential equations are ordinary differential equations whose dependent variables are the partial derivatives of the state variables with respect to the parameters. The sensitivity equations are integrated in parallel with the equations of motion to yield sensitivity coefficients (partial derivatives), which reflect the sensitivity of the computed solution with respect to each aerodynamic coefficient or system parameter (e.g., initial condition).

The use of a truncated Taylor's series expansion brings about a method of quasilinearization which uses these sensitivity coefficients to linearize the change in the solution of the nonlinear equations of motion due to a change in the aerodynamic coefficients or system parameters. As an illustration we will consider the following functional representation of the solution to a system of dynamic equations.

Let:

$\theta_c^0 = f(\vec{c}^0, t)$ = computed solution to the $\ddot{\theta}$ equation of motion based on the initial estimates to the system parameters, $\vec{c}^0$.

$\vec{c} = [c_1, c_2, c_3, \ldots, c_p]^T$ = the system parameter vector containing parameters to be determined.

$\psi_c^0 = g(\vec{c}^0, t)$ = computed solution to the $\ddot{\psi}$ equation of motion based on initial estimates.

$\phi_c^0 = h(\vec{c}^0, t)$ = computed solution to the $\ddot{\phi}$ equation of motion based on initial estimates.

$\theta_E(t)$, $\psi_E(t)$, $\phi_E(t)$ = experimental data at discrete points in time.

Employing a Taylor's series expansion about what will be defined as the nominal solution, and neglecting second and higher order terms results in the following:

$$\theta_c = f\,(\vec{C^O} + \vec{\Delta C},\, t) = f\,(\vec{C^O},\, t) + \sum_{i=1}^{p} \left(\frac{\partial \theta_c^{\,o}}{\partial C_i}\right) \Delta C_i \tag{25}$$

$$\psi_c = g\,(\vec{C^O} + \vec{\Delta C},\, t) = g\,(\vec{C^O},\, t) + \sum_{i=1}^{p} \left(\frac{\partial \psi_c^{\,o}}{\partial C_i}\right) \Delta C_i \tag{26}$$

$$\phi_c = h\,(\vec{C^O} + \vec{\Delta C},\, t) = h\,(\vec{C^O},\, t) + \sum_{i=1}^{p} \left(\frac{\partial \phi_c^{\,o}}{\partial C_i}\right) \Delta C_i \tag{27}$$

Where P is the number of system parameters to be determined. Equations (25) through (27) represent the nominal solution which provides the optimum correlation to the experimental data. Data acquisition errors or measurement noise is defined in Equations (28).

$$R_\theta = \theta_E(t) - \theta_c \tag{28a}$$

$$R_\psi = \psi_E(t) - \phi_c \tag{28b}$$

$$R_\phi = \phi_E(t) - \phi_c \tag{28c}$$

The assumption made is that in the absence of measurement noise, the dynamic equations of motion exactly define the experimental data based on the system parameters, $\vec{c}$. Inclusion of the measurement noise in Equations (25 through 27) gives the following:

$$R_\theta = \theta_E - f\,(\vec{C^O} + \vec{\Delta C},\, t) = \theta_E - f\,(\vec{C^O},\, t) - \sum_{i=1}^{p} \left(\frac{\partial \theta_c^{\,o}}{\partial C_i}\right) \Delta C_i \tag{29a}$$

$$R_\psi = \psi_E - g\,(\vec{C^O} + \vec{\Delta C},\, t) = \psi_E - g\,(\vec{C^O},\, t) - \sum_{i=1}^{p} \left(\frac{\partial \psi_c^{\,o}}{\partial C_i}\right) \Delta C_i \tag{29b}$$

$$R_\phi = \phi_E - h\,(\vec{C^O} + \vec{\Delta C},\, t) = \phi_E - h\,(\vec{C^O},\, t) - \sum_{i=1}^{p} \left(\frac{\partial \phi_c^{\,o}}{\partial C_i}\right) \Delta C_i \tag{29c}$$

Let:

$$E_\theta = \theta_E - f(\vec{C^o}, t) \tag{30a}$$

$$E_\psi = \psi_E - g(\vec{C^o}, t) \tag{30b}$$

$$E_\phi = \phi_E - h(\vec{C^o}, t) \tag{30c}$$

Theoretically R_θ, R_ψ, and R_ϕ have been defined as the measurement noise. In an iterative sense, R is one iteration ahead of E, which is defined in Equations (30). In the limit as convergence is achieved E should approach R being a measure of the measurement noise. E_θ, E_ψ, and E_ϕ can be thought of as an approximation of the measurement noise based on initial estimates, $\vec{c^o}$.

LEAST-SQUARES THEORY

A suitable technique for matching the theoretical trajectory to the actual is least-squares theory. Through successive iterations, the residual functions, R_θ, R_ψ, and R_ϕ, are minimized to the measurement accuracy of the experimental data. The residuals to be minimized are the differences between the experimental data and the computed solution which are defined in the previous section as the measurement noise E. Application of the theory results in the minimization of the squares of the residuals based on variations $(\vec{\Delta c})$ of the system parameters $(\vec{c})$. The square of the residual functions to be minimized are as follows:

$$R_\theta^2 = \sum_{k=1}^{N} [\,\theta_E - f(\vec{C^o} + \vec{\Delta C}, t)\,]_k^2 = \sum_{k=1}^{N} [\, E_\theta - \sum_{i=1}^{p} (\frac{\partial \theta_c^o}{\partial C_i}) \Delta C_i \,]_k^2 \tag{31a}$$

$$R_\psi^2 = \sum_{k=1}^{N} [\,\psi_E - g(\vec{C^o} + \vec{\Delta C}, t)\,]_k^2 = \sum_{k=1}^{N} [\, E_\psi - \sum_{i=1}^{p} (\frac{\partial \psi_c^o}{\partial C_i}) \Delta C_i \,]_k^2 \tag{31b}$$

$$R_\phi^2 = \sum_{k=1}^{N} [\,\phi_E - h(\vec{C^o} + \vec{\Delta C}, t)\,]_k^2 = \sum_{k=1}^{N} [\, E_\phi - \sum_{i=1}^{p} (\frac{\partial \phi_c^o}{\partial C_i}) \Delta C_i \,]_k^2 \tag{31c}$$

Minimization of the sum of the squares of the residuals will be achieved by taking the partial derivative with respect to $\vec{\Delta c}$ and setting it equal to zero. This is indicated in Equations (32). N is defined as the total number of data points.

$$\frac{\partial R_\theta{}^2}{\partial \Delta C_j} = \sum_{k=1}^{N} 2 \left[E_\theta - \sum_{i=1}^{p} \left(\frac{\partial \theta_c{}^o}{\partial C_i}\right) \Delta C_i \right]_k \left[\frac{\partial \theta_c{}^o}{\partial C_j}\right]_k = 0 \tag{32a}$$

$$\frac{\partial R_\psi{}^2}{\partial \Delta C_j} = \sum_{k=1}^{N} 2 \left[E_\psi - \sum_{i=1}^{p} \left(\frac{\partial \psi_c{}^o}{\partial C_i}\right) \Delta C_i \right]_k \left[\frac{\partial \psi_c{}^o}{\partial C_j}\right]_k = 0 \tag{32b}$$

$$\frac{\partial R_\phi{}^2}{\partial \Delta C_j} = \sum_{k=1}^{N} 2 \left[E_\phi - \sum_{i=1}^{p} \left(\frac{\partial \phi_c{}^o}{\partial C_i}\right) \Delta C_i \right]_k \left[\frac{\partial \phi_c{}^o}{\partial C_j}\right]_k = 0 \tag{32c}$$

Equations (32) may be rewritten in matrix notation as follows:

$$[A] = \begin{bmatrix} \dfrac{\partial \theta_c{}^o}{\partial C_1} & \dfrac{\partial \theta_c{}^o}{\partial C_2} & \cdots\cdots\cdots & \dfrac{\partial \theta_c{}^o}{\partial C_p} \\[2mm] \dfrac{\partial \psi_c{}^o}{\partial C_1} & \dfrac{\partial \psi_c{}^o}{\partial C_2} & \cdots\cdots\cdots & \dfrac{\partial \psi_c{}^o}{\partial C_p} \\[2mm] \dfrac{\partial \phi_c{}^o}{\partial C_1} & \dfrac{\partial \phi_c{}^o}{\partial C_2} & \cdots\cdots\cdots & \dfrac{\partial \phi_c{}^o}{\partial C_p} \end{bmatrix}$$

$$[E] = \begin{bmatrix} E_\theta \\ E_\psi \\ E_\phi \end{bmatrix} \qquad\qquad [\Delta C] = \begin{bmatrix} \Delta C_1 \\ \Delta C_2 \\ \cdot \\ \cdot \\ \cdot \\ \Delta C_p \end{bmatrix}$$

$$\sum_{k=1}^{N} [A]^T [A][\Delta C] = \sum_{k=1}^{N} [A]^T [E] \tag{33}$$

Equation (33) may be solved to provide corrections ($[\Delta C]$) to be applied to the aerodynamic coefficients and system parameters ($\widetilde{c}^O$), knowing the partial derivatives ($[A]$ – sensitivity coefficients) and the approximated measurement noise ($[E]$ – e.g. $E_\theta = \theta_E - f(\widetilde{c}^O, t)$).

APPLICATION TO EQUATIONS OF MOTION

In correlating ballistic spark range data using least-squares theory, analysis of the swerve motion (x, y, z) is decoupled from the angular motion (θ, ψ, ϕ). The equations of motion (EOM) used in the decoupled swerve analysis are as follows:

SWERVE EOM

$$\dot{V}_X = (\frac{\rho A V^2}{2m}) [-\overline{C}_x COS\theta_{FP}COS\psi_{FP} - \overline{C}_y (SIN\theta_{FP}COS\psi_{FP}SIN\phi - SIN\psi_{FP}COS\phi) \quad (34a)$$

$$- \overline{C}_z (SIN\theta_{FP}COS\psi_{FP}COS\phi + SIN\psi_{FP}SIN\phi)$$

$$+ \overline{C}_{yp} (\frac{pd}{2V})(SIN\theta_{FP}SIN\phi COS\psi_{FP} - SIN\psi_{FP}COS\phi)$$

$$- \overline{C}_{zp} (\frac{pd}{2V})(SIN\theta_{FP}COS\phi COS\psi_{FP} + SIN\phi SIN\psi_{FP})]$$

$$\dot{V}_Y = (\frac{\rho A V^2}{2m}) [-\overline{C}_x COS\theta_{FP}SIN\psi_{FP} - \overline{C}_y (SIN\theta_{FP}SIN\psi_{FP}SIN\phi + COS\psi_{FP}COS\phi) \quad (34b)$$

$$- \overline{C}_z (SIN\theta_{FP}SIN\psi_{FP}COS\phi - COS\psi_{FP}SIN\phi)$$

$$+ \overline{C}_{yp} (\frac{pd}{2V})(SIN\theta_{FP}SIN\psi_{FP}SIN\phi + COS\psi_{FP}COS\phi)$$

$$- \overline{C}_{zp} (\frac{pd}{2V})(SIN\theta_{FP}SIN\psi_{FP}COS\phi - COS\psi_{FP}SIN\phi)]$$

$$\dot{V}_Z = (\frac{\rho \Lambda V^2}{2m}) \mid -\overline{C}_x SIN\theta_{FP} - \overline{C}_y SIN\phi COS\theta_{FP} \tag{34c}$$

$$-\overline{C}_z COS\phi COS\theta_{FP} + \overline{C}_{yp} (\frac{pd}{2V}) SIN\phi COS\theta_{FP}$$

$$-\overline{C}_{zp} (\frac{pd}{2V}) COS\phi COS\theta_{FP} \mid -g$$

Equations (34) were derived by differentiating the transformation Equations (11a), (11b), and (11c), and substituting Equations (9a), (9b), and (9c) for u_{RB}, v_{RB}, and w_{RB}. Definition of the aerodynamics in Equations (34) follows.

$$\overline{C}_x = C_{xo} + C_{xa2} (\frac{w_{RB}}{V})^2 + C_{x\beta2} (\frac{v_{RB}}{V})^2 + C_{xM} (M - MREF) \tag{35a}$$

$$\overline{C}_y = C_{yo} + C_{y\beta} (\frac{v_{RB}}{V}) + C_{y\beta3} (\frac{v_{RB}}{V})^3 \tag{35b}$$

$$\overline{C}_z = C_{zo} + C_{za} (\frac{w_{RB}}{V}) + C_{za3} (\frac{w_{RB}}{V})^3 \tag{35c}$$

$$\overline{C}_{yp} = C_{ypa} (\frac{w_{RB}}{V}) \tag{35d}$$

$$\overline{C}_{zp} = C_{zp\beta} (\frac{v_{RB}}{V}) \tag{35e}$$

Direct correlation of experimental data to the equations of motion for the determination of the aerodynamic coefficients requires a system of partial differential equations, sometimes called sensitivity equations. This system of equations results from taking partial derivatives with respect to each aerodynamic coefficient on the equations of the motion.

23

The system of partials required for direct correlation to the swerve or position data (x, y, z) is as follows:

$$[A]' = \begin{bmatrix} \dfrac{\partial X}{\partial C_1} & \dfrac{\partial X}{\partial C_2} \cdots\cdots\cdots & \dfrac{\partial X}{\partial C_r} \\[2ex] \dfrac{\partial Y}{\partial C_1} & \dfrac{\partial Y}{\partial C_2} \cdots\cdots\cdots & \dfrac{\partial Y}{\partial C_r} \\[2ex] \dfrac{\partial Z}{\partial C_1} & \dfrac{\partial Z}{\partial C_2} \cdots\cdots\cdots & \dfrac{\partial Z}{\partial C_r} \end{bmatrix} \qquad (36)$$

These partial derivatives are obtained from numerical integration of $\partial \dot{V}_x / \partial C_j$, $\partial \dot{V}_y / \partial C_j$, and $\partial \dot{V}_z / \partial C_j$.

For simplicity of derivation as well as computational purposes, partial derivatives will be stated in generalized form. Derivation of the partial derivative for Equation (34a) follows.

$$\frac{\partial \dot{V}_x}{\partial C_j} = A_1 \frac{\partial V}{\partial C_j} + K_{1j} \frac{\partial C_j}{\partial C_j} \qquad (37)$$

where:

$$A_1 = \frac{\rho A V}{2m} \left[- \left(2C_{xo} + C_{xa2} \left(\frac{w_{RB}}{V}\right)^2 + 2C_{x\beta2} \left(\frac{v_{RB}}{V}\right)^2 + C_{xM}(3M - 2MREF) \right) COS\theta_{FP} COS\psi_{FP} \right.$$

$$- 2 \left(C_{yo} + C_{y\beta} \left(\frac{v_{RB}}{V}\right) + C_{y\beta3} \left(\frac{v_{RB}}{V}\right)^3 \right) (SIN\theta_{FP} COS\psi_{FP} SIN\phi - SIN\psi_{FP} COS\phi)$$

$$- 2 \left(C_{zo} + C_{za} \left(\frac{w_{RB}}{V}\right) + C_{za3} \left(\frac{w_{RB}}{V}\right)^3 \right) (SIN\theta_{FP} COS\psi_{FP} COS\phi + SIN\psi_{FP} SIN\phi)$$

$$+ C_{ypa} \left(\frac{w_{RB}}{V}\right) \left(\frac{pd}{2V}\right) (SIN\theta_{FP} SIN\phi COS\psi_{FP} - SIN\psi_{FP} COS\phi)$$

$$\left. - C_{zp\beta} \left(\frac{v_{RB}}{V}\right) \left(\frac{pd}{2V}\right) (SIN\theta_{FP} COS\phi COS\psi_{FP} + SIN\phi SIN\psi_{FP}) \right]$$

24

$$e.g. \quad K_1 = -\frac{\rho A V^2}{2m} \left(\frac{w_{RB}}{V}\right)^3 \quad (SIN\theta_{FP}COS\psi_{FP}COS\phi + SIN\psi_{FP}SIN\phi)$$

for j corresponding to $C_{z\alpha3}$

$$V = (V_x^2 + V_y^2 + V_z^2)^{1/2}$$

$$\frac{\partial V}{\partial C_j} = \frac{V_x}{V} \frac{\partial V_x}{\partial C_j} + \frac{V_y}{V} \frac{\partial V_y}{\partial C_j} + \frac{V_z}{V} \frac{\partial V_z}{\partial C_j}$$

As indicated in the preceding partial derivative, those variables computed during analysis of the angular motion are assumed known and therefore, are not treated as dependent variables. The variables which are assumed known are w_{RB}/V, v_{RB}/V, θ_{FP}, ψ_{FP}, and ϕ. Derivation of the complete set of partial derivatives used for analysis of the position data is contained in Appendix A.

The equations of motion used in the angular motion analysis are as follows:

ANGULAR EOM

$$\dot{p} = \frac{I_y L_p + I_{xy} L_q - (I_x + I_y - I_z) I_{xy} pr + (I_{xy}^2 + I_y (I_y - I_z)) qr}{(I_x I_y - I_{xy}^2)} \tag{38a}$$

$$\dot{q} = \frac{I_x L_q + I_{xy} L_p + (I_x + I_y - I_z) I_{xy} qr + (I_x (I_z - I_x) - I_{xy}^2) pr}{(I_x I_y - I_{xy}^2)} \tag{38b}$$

$$\dot{r} = \frac{L_r + I_{xy} (p^2 - q^2) + (I_x - I_y) pq}{I_z} \tag{38c}$$

$$\dot{v}_{RB} = pw_{RB} - ru_{RB} + F_y/m - g \, SIN\phi COS\theta_{FP} \tag{38d}$$

$$\dot{w}_{RB} = qu_{RB} - pv_{RB} + F_z/m - g \, COS\phi COS\theta_{FP} \tag{38e}$$

$$\dot{\phi} = p + TAN\theta_{FP} (q \, SIN\phi + r \, COS\phi) \tag{38f}$$

$$\dot{\theta} = q \, COS\phi - r \, SIN\phi \tag{38g}$$

The $\dot{\psi}$ equation is not included since ψ_{FP} and $\dot{\psi}$ are not needed for the analysis.

25

Definition of the aerodynamics in Equations (38) follows.

$$L_p = \bar{q}Ad \left[C_{\ell\delta} + C_{\ell p} \left(\frac{pd}{2V}\right) + C_{\ell\phi} \ SIN^2 \ \bar{a} \ SIN \ (n\phi') \right] \tag{39a}$$

$$L_q = \bar{q}Ad \left[C_{mo} + C_{ma} \left(\frac{w_{RB}}{V}\right) + C_{ma3} \left(\frac{w_{RB}}{V}\right)^3 + C_{mq} \left(\frac{qd}{2V}\right) + C_{mq2} \left(\frac{qd}{2V}\right)\left(\frac{w_{RB}}{V}\right)^2 \right. \tag{39b}$$

$$+ C_{mp\beta} \left(\frac{pd}{2V}\right)\left(\frac{v_{RB}}{V}\right) + C_{m\phi a} SIN^2 \ \bar{a} \ SIN \ (n\phi')\left(\frac{w_{RB}}{V}\right)$$

$$\left. + C_{n\phi a} \ SIN^2 \ \bar{a} \ SIN \ (n\phi')\left(\frac{v_{RB}}{V}\right) \right]$$

$$L_r = \bar{q}Ad \left[C_{no} + C_{n\beta} \left(\frac{v_{RB}}{V}\right) + C_{n\beta3} \left(\frac{v_{RB}}{V}\right)^3 + C_{nr} \left(\frac{rd}{2V}\right) \right. \tag{39c}$$

$$+ C_{nr2} \left(\frac{rd}{2V}\right) \left(\frac{v_{RB}}{V}\right)^2 + C_{npa} \left(\frac{pd}{2V}\right)\left(\frac{w_{RB}}{V}\right) - C_{m\phi a} SIN^2 \ \bar{a} \ SIN(n\phi')\left(\frac{v_{RB}}{V}\right)$$

$$\left. + C_{n\phi a} SIN^2 \ \bar{a} \ SIN(n\phi')\left(\frac{w_{RB}}{V}\right) \right]$$

$$F_Y = \bar{q}A \left[C_{yo} + C_{y\beta} \left(\frac{v_{RB}}{V}\right) + C_{y\beta3} \left(\frac{v_{RB}}{V}\right)^3 + C_{ypa} \left(\frac{pd}{2V}\right)\left(\frac{w_{RB}}{V}\right) \right. \tag{39d}$$

$$\left. - C_{N\phi a} SIN^2 \ \bar{a} \ SIN(n\phi') \left(\frac{v_{RB}}{V}\right) + C_{y\phi a} SIN^2 \ \bar{a} \ SIN(n\phi')\left(\frac{w_{RB}}{V}\right) \right]$$

$$F_Z = \bar{q}A \left[C_{zo} + C_{za} \left(\frac{w_{RB}}{V}\right) + C_{za3} \left(\frac{w_{RB}}{V}\right)^3 + C_{zp\beta} \left(\frac{pd}{2V}\right)\left(\frac{v_{RB}}{V}\right) \right. \tag{39e}$$

$$\left. - C_{N\phi a} SIN^2 \ \bar{a} \ SIN(n\phi') \left(\frac{w_{RB}}{V}\right) - C_{y\phi a} SIN^2 \ \bar{a} \ SIN(n\phi')\left(\frac{v_{RB}}{V}\right) \right]$$

The system of partial differential equations required for direct correlation to the angular motion data (θ_{RB}, ψ_{RB}, ϕ) is as follows:

$$[\,B\,] = \begin{bmatrix} \dfrac{\partial \theta_{RB}}{\partial C_1} & \dfrac{\partial \theta_{RB}}{\partial C_2} & \cdots\cdots\cdots & \dfrac{\partial \theta_{RB}}{\partial C_s} \\[3ex] \dfrac{\partial \psi_{RB}}{\partial C_1} & \dfrac{\partial \psi_{RB}}{\partial C_2} & \cdots\cdots\cdots & \dfrac{\partial \psi_{RB}}{\partial C_s} \\[3ex] \dfrac{\partial \phi}{\partial C_1} & \dfrac{\partial \phi}{\partial C_2} & \cdots\cdots\cdots & \dfrac{\partial \phi}{\partial C_s} \end{bmatrix} \tag{40}$$

These partials are obtained from numerical integration of $\partial \dot{v}_{RB}/\partial C_j$, $\partial \dot{w}_{RB}/\partial C_j$, $\partial \phi/\partial C_j$. Having obtained $\partial v_{RB}/\partial C_j$ and $\partial w_{RB}/\partial C_j$, the transformation equations are used to obtain partials of θ_{RB} and ψ_{RB} as follows:

$$\psi_{RB} = -\,\mathrm{SIN}^{-1}\,(\,v_{RB}/V) \tag{41a}$$

$$\theta_{RB} = \mathrm{SIN}^{-1}\,(w_{RB}/(V\mathrm{COS}\psi_{RB})) \tag{41b}$$

Using the chain differentiation rule results in the following:

$$\frac{\partial \theta_{RB}}{\partial C_j} = \frac{\partial v_{RB}}{\partial C_j}\,\frac{\partial \theta_{RB}}{\partial v_{RB}} + \frac{\partial w_{RB}}{\partial C_j}\,\frac{\partial \theta_{RB}}{\partial w_{RB}} \tag{42a}$$

$$\frac{\partial \psi_{RB}}{\partial C_j} = \frac{\partial v_{RB}}{\partial C_j}\,\frac{\partial \psi_{RB}}{\partial v_{RB}} + \frac{\partial w_{RB}}{\partial C_j}\,\frac{\partial \psi_{RB}}{\partial w_{RB}} \tag{42b}$$

The derivatives of Equations (41) are:

$$\frac{\partial \psi_{RB}}{\partial w_{RB}} = 0.0 \tag{43a}$$

$$\frac{\partial \psi_{RB}}{\partial v_{RB}} = -\,\frac{1}{(V^2 - v_{RB}^2)^{1/2}} \tag{43b}$$

$$\frac{\partial \theta_{RB}}{\partial w_{RB}} = \frac{1}{(V^2\mathrm{COS}^2\psi_{RB} - w_{RB}^2)^{1/2}} \tag{43c}$$

$$\frac{\partial \theta_{RB}}{\partial v_{RB}} = \left[\frac{1}{(V^2 COS^2 \psi_{RB} - w_{RB}^2)^{1/2}} \right] \left[-\frac{w_{RB}}{COS \psi_{RB}} \right] \left[\frac{SIN \psi_{RB}}{(V^2 - v_{RB}^2)^{1/2}} \right] \qquad (43d)$$

Equations (43) are substituted into Equations (42) to obtain $\partial \theta_{RB}/\partial C_j$ and $\partial \psi_{RB}/\partial C_j$ which are used to form the matrix [B], Equation (40). The system of correction equations used to correlate the angular motion data is stated as follows in matrix notation.

$$[B]^T [W] [B] [\Delta C] = [B]^T [W] [R]$$

$$[W] = \begin{bmatrix} 1 & 0 & 0 \\ 0 & 1 & 0 \\ 0 & 0 & W_3 \end{bmatrix} \qquad (44)$$

Equation (44) represents a weighted least squares formulation to correlate θ_{RB}, ψ_{RB}, and ϕ. The [W] matrix is used to weight the correlation of ϕ since the measurement errors on ϕ are of the order of 5 to 10 times larger than θ_{RB} and ψ_{RB}.

where:

$$W_3 = \text{weighting factor on } \phi$$

Derivation of the partial derivatives for Equations (38) is contained in Appendix A. The velocity is assumed known from analysis of the swerve motion and is therefore not treated as a dependent variable.

The yaw data correlated during analysis of the angular motion, θ_{RB} and ψ_{RB}, is transformed after the swerve analysis as follows:

$$v_{RB} = V_X [SIN\theta_{FP}SIN\phi COS\psi_{FP} - COS\phi SIN\psi_{FP}] \qquad (45a)$$

$$+ V_Y [SIN\theta_{FP}SIN\phi SIN\psi_{FP} + COS\phi COS\psi_{FP}]$$

$$+ V_Z SIN\phi COS\theta_{FP}$$

$$w_{RB} = V_X [SIN\theta_{FP}COS\phi COS\psi_{FP} + SIN\phi SIN\psi_{FP}] \qquad (45b)$$

$$+ V_Y [SIN\theta_{FP}COS\phi SIN\psi_{FP} - SIN\phi COS\psi_{FP}]$$

$$+ V_Z COS\phi COS\theta_{FP}$$

28

$$\psi_{RB} = -SIN^{-1} (v_{RB}/V) \tag{45c}$$

$$\theta_{RB} = SIN^{-1} \left[\frac{w_{RB}}{VCOS\psi_{RB}}\right] \tag{45d}$$

In summation, the measured six-degree-of-freedom data $(X, Y, Z, \theta_{FP}, \psi_{FP}, \phi)$ are correlated as follows. The position data are fit to Equations (34) resulting in a determination of the aerodynamic force coefficients. The yaw data $(\theta_{FP}$ and $\psi_{FP})$ are then transformed to the body-fixed coordinate system using the computed earth-fixed velocity components, V_X, V_Y, and V_Z. Equations (45) are the transformation equations used. The angular motion data $(\theta_{RB}, \psi_{RB}, \phi)$ are then analyzed using Equations (38) to result in a determination of the aerodynamic moment coefficients. A weighted least squares formulation is used to account for the larger measurement errors in ϕ relative to θ_{RB} and ψ_{RB}.

SECTION IV

PROGRAM UTILIZATION

Data acquired from the Eglin Aeroballistic Range Facility consist of photographic records of the angular and linear position of a body in free flight. The photographs are taken from surveyed stations spaced on the order of 5 to 20-foot intervals along the length of the range. The records are obtained from dual-axis spark shadowgraphs. Optical axes at each shadowgraph station are mutually orthogonal with the range centerline. A film reader is used to result in numerical interpretations of the shadowgrams which provides histories of attitude and position as functions of time $(X, Y, Z, \theta_{FP}, \psi_{FP}, \phi$ vs. time).

The six-degree-of-freedom data is then correlated to the equations of motion as derived in the body-fixed coordinate system. The aerodynamic model used is derived in Section II and the data correlation technique is detailed in Section III.

REDUCTION PROCEDURE

The normal reduction sequence to determine the force and moment coefficients consists of the execution of five computer programs. The final two computer programs are for simultaneous reduction of up to three rounds of similar configurations. Figure 6 represents a basic block diagram of the reduction sequence illustrating the flow of information between programs. A description of the function of each program follows.

ROLLNUT
- Preliminary transformation from earth fixed to missile angles.
- Fits missile angles using modified linear theory.
- Computes dense profile (relative to data profile) of body-fixed angles and angular rates from approximate transformations for use in ROLL-HEEVE.
- Computes initial conditions for ROLL-HEEVE and ROLL-ANGLES.

ROLL-HEEVE
- Provides a best fit to the position data using earth fixed equations of motion.
- Provides a preliminary fit to the roll data (ϕ) assuming $I_{xy} = 0$.

30
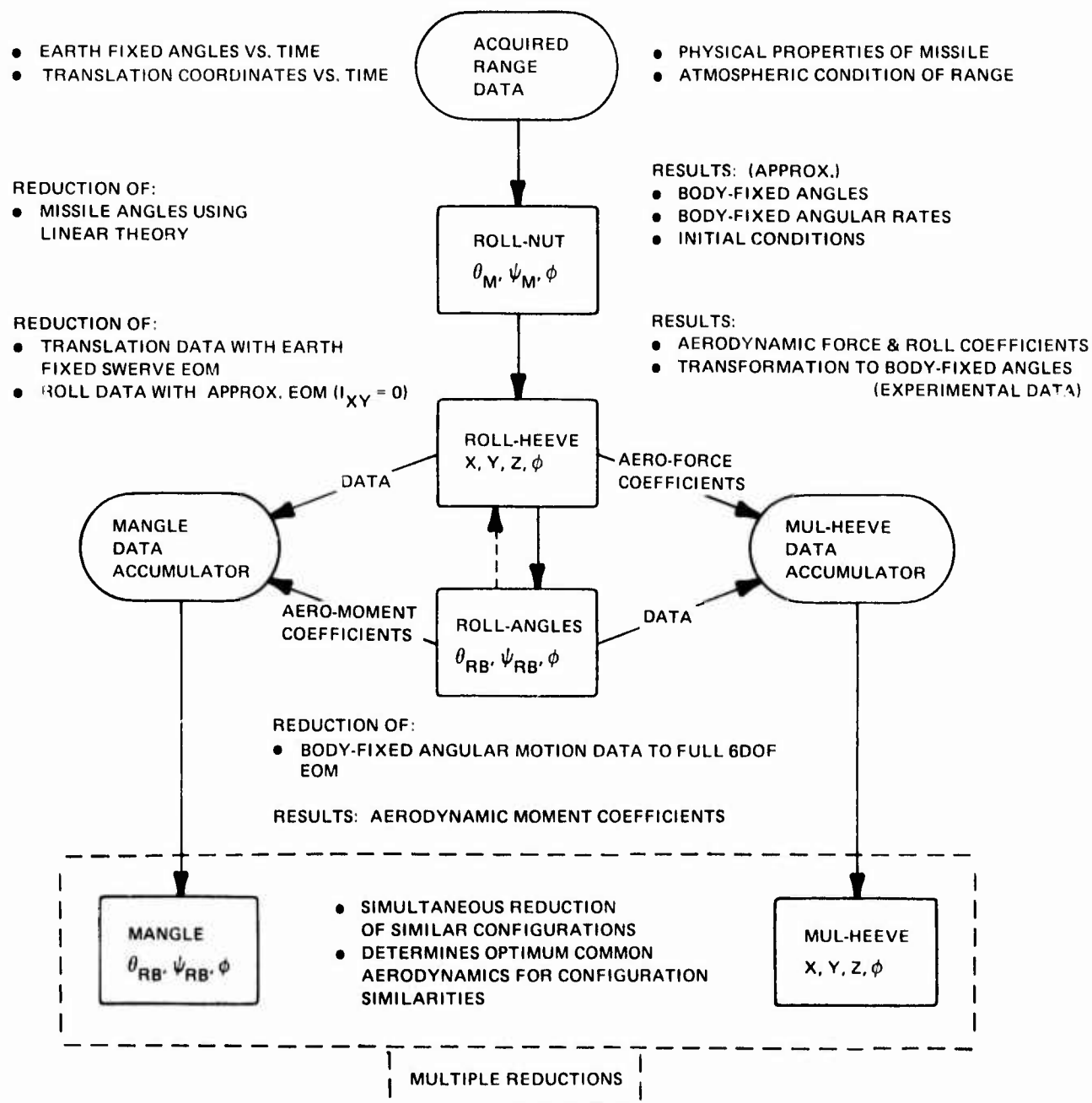
Figure 6. Body-Fixed Data Analysis System

- Transforms the fixed-plane angle data (ϕ_{FP}, ψ_{FP}) to body-fixed angles (θ_{RB}, ψ_{RB}) using the computed earth-fixed velocity components and experimental roll data.
- The total velocity profile is computed for use in ROLL-ANGLES.
- Results in the aerodynamic force and roll moment coefficients.

ROLL-ANGLES
- Provides a best fit to the angular motion data (θ_{RB}, ψ_{RB}, ϕ) using the body-fixed equations of motion.
- Computes a dense profile of the body-fixed angles and angular rates for a final swerve analysis (ROLL-HEEVE).
- Results in the aerodynamic moment coefficients.

MANGLE
- Simultaneous angular reduction of up to three data sets from similar configurations.
- Determines optimum common aerodynamics corresponding to configuration similarities and unique coefficients per data set to those parameters which are not common.

MUL-HEEVE
- Simultaneous swerve reduction of up to three data sets from similar configurations.
- Determines optimum common aerodynamic force coefficients corresponding to configuration similarities and unique coefficients per data set to those parameters which are not common.

The input required to execute each program is defined in Appendix B.

During implementation of the derived model (equations of motion) and data correlation technique, options were included such that the data analysis could be made using symmetric aerodynamics. These options exist in the form of an additional set of aerodynamic coefficients paralleling those derived in Section II. For example, the pitching moment coefficients C_{ma} and $C_{n\beta}$ are paralleled by $C_{m\bar{a}}$ which is the symmetric pitching moment term. The purpose of these options is three-fold. If the data being analyzed is on a symmetric configuration, then the symmetric aerodynamics should be computed while setting the nonsymmetric coefficients to zero. Secondly, if only slight asymmetries are present in certain forces and moments and the quality of the data is not good enough to determine the asymmetric effects, then the forces and moments may be constrained to be equal in each of the body-fixed planes by using the symmetric terms. Finally, when initial estimates of the aerodynamics are not very good, initial execution of the programs should be done using the symmetric terms such that convergence will be assured and improved initial estimates determined for the final analysis. A definition of the complete set of aerodynamic coefficients and equations of motion for each program follows.

32

The program ROLL-HEEVE which does the swerve analysis includes a preliminary analysis of the roll data. The equation of motion was simplified by assuming I_{xy} equal to zero. This correlation of the roll data is done independently of the correlation to the position data.

The sign convention of the aerodynamic coefficients in some cases differs from the derivation. The signs reflected in the following equations are exactly as programmed. The user is advised to use these equations to verify the sign convention of determined coefficients resulting from the computer programs.

ROLL-NUT Equations of Motion

$$\theta_m = K_1 e^{\lambda_1 X} \text{SIN} (\phi_1 + \omega_1 X + \dot{\omega}_1 X^2/2)$$

$$+ K_2 e^{\lambda_2 X} \text{SIN} (\phi_2 + \omega_2 X + \dot{\omega}_2 X^2/2)$$

$$+ K_3 \text{SIN} (\phi_3 + \phi)$$

$$\psi_m = K_1 e^{\lambda_1 X} \text{COS} (\phi_1 + \omega_1 X + \dot{\omega}_1 X^2/2)$$

$$+ K_2 e^{\lambda_2 X} \text{COS} (\phi_2 + \omega_2 X + \dot{\omega}_2 X^2/2)$$

$$+ K_3 \text{COS} (\phi_3 + \phi)$$

Parameters to be determined from correlation:

K_1	=	nutation amplitude vector, degrees
λ_1	=	nutation damping exponent
ϕ_1	=	initial orientation of nutation vector, degrees
ω_1	=	nutation frequency, deg/ft
$\dot{\omega}_1$	=	rate of change of nutation frequency, deg/ft^2
K_2	=	precession amplitude vector, degrees
λ_2	=	precession damping exponent
ϕ_2	=	initial orientation of precession vector, degrees
ω_2	=	precession frequency, deg/ft
$\dot{\omega}_2$	=	rate of change of precession frequency, deg/ft^2
K_3	=	trim amplitude vector, degrees
ϕ_3	=	initial orientation of trim vector, degrees

34

$$\dot{V}_x = (\frac{\rho A V^2}{2m}) \, [\, -\overline{C}_x COS\theta_{FP} COS\psi_{FP} - \overline{C}_y \, (SIN\theta_{FP} COS\psi_{FP} SIN\phi - SIN\psi_{FP} COS\phi)$$

$$- \overline{C}_z \, (SIN\theta_{FP} COS\psi_{FP} COS\phi + SIN\psi_{FP} SIN\phi)$$

$$+ \overline{C}_{yp} \, (\frac{pd}{2V}) \, (SIN\theta_{FP} SIN\phi COS\psi_{FP} - SIN\psi_{FP} COS\phi)$$

$$- \overline{C}_{zp} \, (\frac{pd}{2V}) \, (SIN\theta_{FP} COS\phi COS\psi_{FP} + SIN\phi SIN\psi_{FP}) \,]$$

$$\dot{V}_y = (\frac{\rho A V^2}{2m}) \, [\, -\overline{C}_x COS\theta_{FP} SIN\psi_{FP} - \overline{C}_y \, (SIN\theta_{FP} SIN\psi_{FP} SIN\phi + COS\psi_{FP} COS\phi)$$

$$- \overline{C}_z \, (SIN\theta_{FP} SIN\psi_{FP} COS\phi - COS\psi_{FP} SIN\phi)$$

$$+ \overline{C}_{yp} \, (\frac{pd}{2V}) \, (SIN\theta_{FP} SIN\psi_{FP} SIN\phi + COS\psi_{FP} COS\phi)$$

$$- \overline{C}_{zp} \, (\frac{pd}{2V}) \, (SIN\theta_{FP} SIN\psi_{FP} COS\phi - COS\psi_{FP} SIN\phi) \,]$$

$$\dot{V}_z = (\frac{\rho A V^2}{2m}) \, [\, -\overline{C}_x SIN\theta_{FP} - \overline{C}_y SIN\phi COS\theta_{FP}$$

$$- \overline{C}_z COS\phi COS\theta_{FP} + \overline{C}_{yp} \, (\frac{pd}{2V}) \, SIN\phi COS\theta_{FP}$$

$$- \overline{C}_{zp} \, (\frac{pd}{2V}) \, COS\phi COS\theta_{FP} \,] - g$$

$$\dot{P} = (\frac{\overline{q} A d}{I_x}) \, [\, (\frac{pd}{2V}) \, C_{\ell p} + C_{\ell \delta} + C_{\ell \phi} SIN^2 \overline{a} \, SIN(n\phi') \,] + (\frac{I_y - I_z}{I_x}) \, qr$$

$$\dot{\phi} = p + TAN\theta_{FP} \, (q \, SIN\phi + r \, COS\phi)$$

where:

n = no. of fins, i.e., no. of symmetries

$$\phi' = TAN^{-1} \left(\frac{v_{RB}}{w_{RB}} \right)$$

$$\overline{C}_x = C_{xo} + C_{xa2} \left(\frac{w_{RB}}{V} \right)^2 + C_{x\beta 2} \left(\frac{v_{RB}}{V} \right)^2 + C_{xM} (M - MREF) + \boxed{C_{x\overline{a}2} SIN^2 \overline{a}}$$

$$\overline{C}_y = C_{yo} + C_{y\beta} \left(\frac{v_{RB}}{V} \right) + C_{y\beta 3} \left(\frac{v_{RB}}{V} \right)^3 + \boxed{C_{N\overline{a}} \left(\frac{v_{RB}}{V} \right) + C_{N\overline{a}3} SIN^2 \overline{a} \left(\frac{v_{RB}}{V} \right)}$$

$$\overline{C}_z = C_{zo} + C_{za} \left(\frac{w_{RB}}{V} \right) + C_{za3} \left(\frac{w_{RB}}{V} \right)^3 + \boxed{C_{N\overline{a}} \left(\frac{w_{RB}}{V} \right) + C_{N\overline{a}3} SIN^2 \overline{a} \left(\frac{w_{RB}}{V} \right)}$$

$$C_{yp} = C_{ypa} \left(\frac{w_{RB}}{V} \right) + \boxed{C_{yp\overline{a}} \left(\frac{w_{RB}}{V} \right)}$$

$$C_{zp} = C_{zp\beta} \left(\frac{v_{RB}}{V} \right) + \boxed{C_{yp\overline{a}} \left(\frac{v_{RB}}{V} \right)}$$

$$\boxed{} - \text{SYMMETRY TERMS}$$

$$\dot{p} = \frac{-[(I_x + I_y - I_z) I_{xy}] pr + [I_{xy}^2 + I_y (I_y - I_z)] qr + I_y L_p + I_{xy} L_q}{(I_x I_y - I_{xy}^2)}$$

$$\dot{q} = \frac{[(I_x + I_y - I_z) I_{xy}] qr - [I_{xy}^2 + I_x (I_x - I_z)] pr + I_{xy} L_p + I_x L_q}{(I_x I_y - I_{xy}^2)}$$

$$\dot{r} = \frac{I_{xy} (p^2 - q^2) + (I_x - I_y) pq + L_r}{I_z}$$

$$\dot{\phi} = p + TAN\theta_{FP} (q\ SIN\phi + r\ COS\phi)$$

$$\dot{\theta} = q\ COS\phi - r\ SIN\phi$$

$$\dot{v} = -g\ SIN\phi COS\theta_{FP} - ru_{RB} + pw_{RB} + F_y/m$$

$$\dot{w} = -g\ COS\phi COS\theta_{FP} - pv_{RB} + qu_{RB} + F_z/m$$

$$F_y = \bar{q}AC_Y$$

$$F_z = \bar{q}AC_Z$$

$$L_p = \bar{q}AdC_l$$

$$L_q = \bar{q}AdC_m$$

$$L_r = \bar{q}AdC_n$$

$$\bar{q} = 1/2\ \rho\ V^2$$

37

where:

Normal Type

$$C_Y = -C_{YO} - C_{Y\beta}\left(\frac{^V RB}{V}\right) - C_{Y\beta 3}\left(\frac{^V RB}{V}\right)^3 \left[-C_{N\bar{a}}\left(\frac{^V RB}{V}\right) - C_{N\bar{a}3} \mathrm{SIN}^2\, \bar{a}\left(\frac{^V RB}{V}\right) \right]$$

Magnus Type

$$+ C_{Ypa}\left(\frac{pd}{2V}\right)\left(\frac{^W RB}{V}\right) \left[+ C_{Yp\bar{a}}\left(\frac{pd}{2V}\right)\left(\frac{^W RB}{V}\right) \right]$$

Induced Normal*

$$- C_{N\phi\bar{a}} \;\; \mathrm{SIN}\,(n\phi')\,\mathrm{SIN}^2\, \bar{a}\left(\frac{^V RB}{V}\right)$$

Induced Side*

$$+ C_{Y\phi\bar{a}} \;\; \mathrm{SIN}\,(n\phi')\,\mathrm{SIN}^2\, \bar{a}\left(\frac{^W RB}{V}\right)$$

Normal Type

$$C_Z = - C_{ZO} - C_{Za}\left(\frac{^W RB}{V}\right) - C_{Za3}\left(\frac{^W RB}{V}\right)^3 \left[- C_{N\bar{a}}\left(\frac{^W RB}{V}\right) - C_{N\bar{a}3} \mathrm{SIN}^2\, \bar{a}\left(\frac{^W RB}{V}\right) \right]$$

Magnus Type

$$C_{Zp\beta}\left(\frac{pd}{2V}\right)\left(\frac{^V RB}{V}\right) \left[- C_{Yp\bar{a}}\left(\frac{pd}{2V}\right)\left(\frac{^V RB}{V}\right) \right]$$

Induced Normal*

$$C_{N\phi\bar{a}} \,\mathrm{SIN}\,(n\phi')\,\mathrm{SIN}^2\, \bar{a}\left(\frac{^W RB}{V}\right)$$

Induced Side*

$$C_{Y\phi\bar{a}} \,\mathrm{SIN}\,(n\phi')\,\mathrm{SIN}^2\, \bar{a}\left(\frac{^V RB}{V}\right)$$

* Not included in current program.

[ ] SYMMETRY TERMS

Pitching

$$C_m = C_{mo} + C_{ma} (\frac{w_{RB}}{V}) + C_{ma3} (\frac{w_{RB}}{V})^3 + \left[C_{m\bar{a}} (\frac{w_{RB}}{V}) + C_{m\bar{a}3} SIN^2 \bar{a} (\frac{w_{RB}}{V}) \right]$$

Damping

$$+ C_{mq} (\frac{qd}{2V}) + C_{mq2} (\frac{qd}{2V}) (\frac{w_{RB}}{V})^2 + \left[C_{m\bar{q}} (\frac{qd}{2V}) + C_{m\bar{q}2} (\frac{qd}{2V}) SIN^2 \bar{a} \right]$$

Magnus

$$+ C_{mp\beta} (\frac{pd}{2V}) (\frac{v_{RB}}{V}) + \left[C_{np\bar{a}} (\frac{pd}{2V}) (\frac{v_{RB}}{V}) \right]$$

Induced Pitching
(freq. effect)

$$+ C_{m\phi\bar{a}} SIN (n\phi') SIN^2 \bar{a} (\frac{w_{RB}}{V})$$

Induced Side Moment
(damping effect)

$$+ C_{n\phi\bar{a}} SIN (n\phi') SIN^2 \bar{a} (\frac{v_{RB}}{V})$$

Pitching

$$C_n = C_{no} - C_{n\beta} (\frac{v_{RB}}{V}) - C_{n\beta3} (\frac{v_{RB}}{V})^3 - \left[C_{m\bar{a}} (\frac{v_{RB}}{V}) - C_{m\bar{a}} SIN^2 \bar{a} (\frac{v_{RB}}{V}) \right]$$

Damping

$$+ C_{nr} (\frac{rd}{2V}) + C_{nr2} (\frac{rd}{2V}) (\frac{v_{RB}}{V})^2 + \left[C_{m\bar{q}} (\frac{rd}{2V}) + C_{m\bar{q}2} (\frac{rd}{2V}) SIN^2 \bar{a} \right]$$

Magnus

$$+ C_{npa} (\frac{pd}{2V}) (\frac{w_{RB}}{V}) + \left[C_{np\bar{a}} (\frac{pd}{2V}) (\frac{w_{RB}}{V}) \right]$$

Induced Pitching
(freq. effect)

$$- C_{m\phi\bar{a}} SIN (n\phi') SIN^2 \bar{a} (\frac{v_{RB}}{V})$$

Induced Side
(damping effect)

$$+ C_{n\phi\bar{a}} SIN (n\phi') SIN^2 \bar{a} (\frac{w_{RB}}{V})$$

Roll Trim

$$C_\ell = C_{\ell\delta}$$

Spin Decay

$$+ C_{\ell p} (\frac{pd}{2V})$$

$$\boxed{} - \text{SYMMETRY TERMS}$$

Induced Roll

$$+ C_{\ell\phi} SIN^2 \bar{a} SIN (n\phi')$$

SECTION V

DATA ANALYSIS RESULTS

Since the model derived in Section II represents a large class of flying objects, it is necessary to extract by coefficient variation that one which corresponds to the actual missile as observed by tests, specifically the free flight motion of a nonsymmetric body. The basic form of the body-fixed six-degree-of-freedom equations of motion is common to the field of Free Flight Dynamics. The basic aerodynamic forces and moments assumed to be acting on a nonsymmetric body as discussed in Section II have been used in missile and aircraft design. Modeling of the nonlinearities in the forces and moments as well as induced effects is not nearly as common and is difficult to determine from the literature.

Preliminary checking of the programs described in the previous section was achieved utilizing an ideal test case generated using a six-degree-of-freedom trajectory program. The test case was essentially that of a symmetric cone. The purpose of using such a test case was that during development and implementation of the programs a major concern in verification was to insur that the transformations were correct in going to body-fixed coordinates, the differential corrections procedure was properly implemented, and in general the entire reduction procedure was consistent. This approach proved valuable towards preliminary verification in solving problems during implementation.

Ballistic spark range data on two elliptic cones were provided by AEDC for analysis. The cones had non-equal transverse inertias ($I_y \neq I_z$) which provides an indication of the asymmetry involved. The physical properties are tabulated in Table 1. Correlation of the free flight range data to the six-degree-of-freedom equations of motion was done using the reduction procedure detailed in Section IV. The results of the analysis are tabulated in Table 2. These aerodynamic coefficients result in a probable error of fit to the data which is about equivalent to the acquisition errors. The elliptic cone was treated as a two fin configuration for the induced effects since a plane of symmetry is encountered every 180 degrees. The maximum yaws for the two elliptic cones were about 6 and 3 degrees for Cones No. 1 and 2 respectively. Figures 7 and 8 illustrate the free flight angular motion of each cone as plotted in the body-fixed coordinate system. These plots illustrate the correlation to the angular motion data resulting from single reduction fits. Figure 9 illustrates the fixed plane angular motion of Cone No. 1.

40

TABLE 1. PHYSICAL PROPERTIES

CONE NO.	Vm (Ft/sec)	DIAM. (Inches)	LENGTH (Inches)	WEIGHT (Pounds)	I_x (Lb-in^2)	I_y (Lb-in^2)	I_z (Lb-in^2)	I_{xy} (Lb-in^2)
1	8410.	1.484	4.704	0.2293	0.04158	0.35180	0.33933	0.
2	8395.	1.484	4.699	0.2338	0.04220	0.35640	0.34350	0.

41

TABLE 2.   DATA ANALYSIS RESULTS

SWERVE REDUCTION

| CONE NO. | PROBABLE ERROR | | C_{xo} | C_{xa2} | $C_{x\beta2}$ | C_{yo} | $C_{y\beta}$ | C_{zo} | C_{za} | C_{ypa} |
	x	y-z								
1	0.0024'	0.0066'	0.0851	.516	1.577	–	2.030	–	1.043	−0.9*
2	0.0020'	0.0014'	0.0860	C_{xa2} 3.0*	–	−0.001	2.298	0.0015	1.605	−0.9*
SIMULTANEOUS FIT 1,2	0.0020'	0.0048'	0.0890	0.508	0.562	(1) – (2) −0.00015	2.029	(1) – (2) −0.00039	1.147	−0.9*

ANGULAR MOTION

| CONE NO. | PROBABLE ERROR | | C_{mo} | C_{ma} | C_{no} | $C_{n\beta}$ | $C_{m\phi a}$ | C_{mq} | C_{npa} | $C_{\ell p}$ | $C_{\ell\delta}$ | $C_{\ell\phi}$ |
	θ_{RB}-V_{RB}	ϕ										
1	0.109°	0.766°	.00114	−0.3048	−0.00008	−0.4031	0.4463	−3.38	−0.05*	−0.002*	−0.00005	0.3488
2	0.094°	0.474°	−.00126	−0.3095	−0.00116	−0.3828	–	−2.89	−0.05*	−0.002*	0.0001	0.6230
SIMULTANEOUS FIT 1,2	0.093°	1.21°	(1) .00111 (2) −.00122	−0.3066	(1) −0.00006 (2) −0.00117	−0.4025	0.431	−3.20	−0.05*	−0.002*	−0.00004	0.3477

* - HELD CONSTANT.

42

Figure 7. θ_{RB} versus ψ_{RB}

Figure 8. θ_{RB} versus ψ_{RB}

44

Figure 9. θ_{FP} versus ψ_{FP}

45
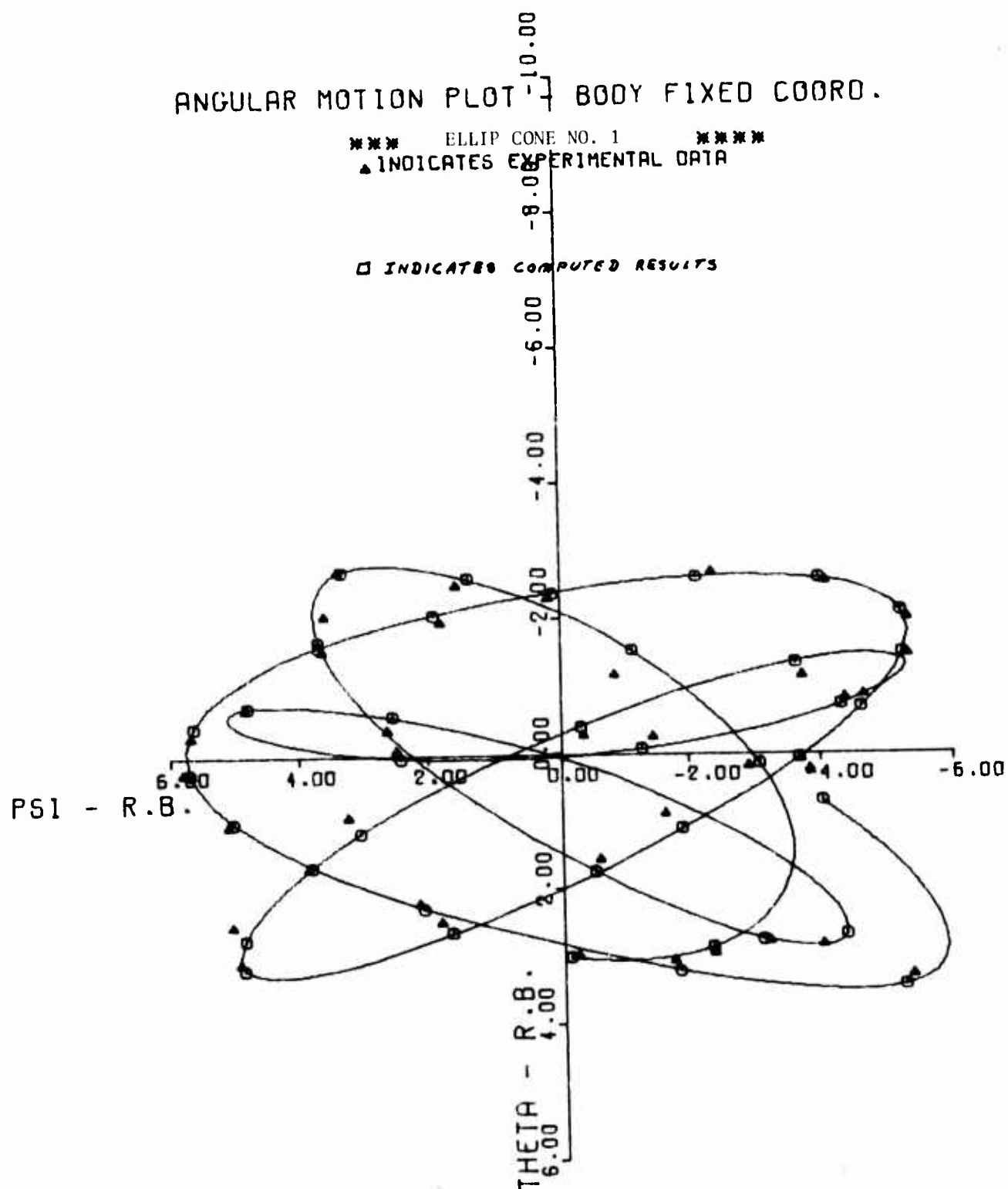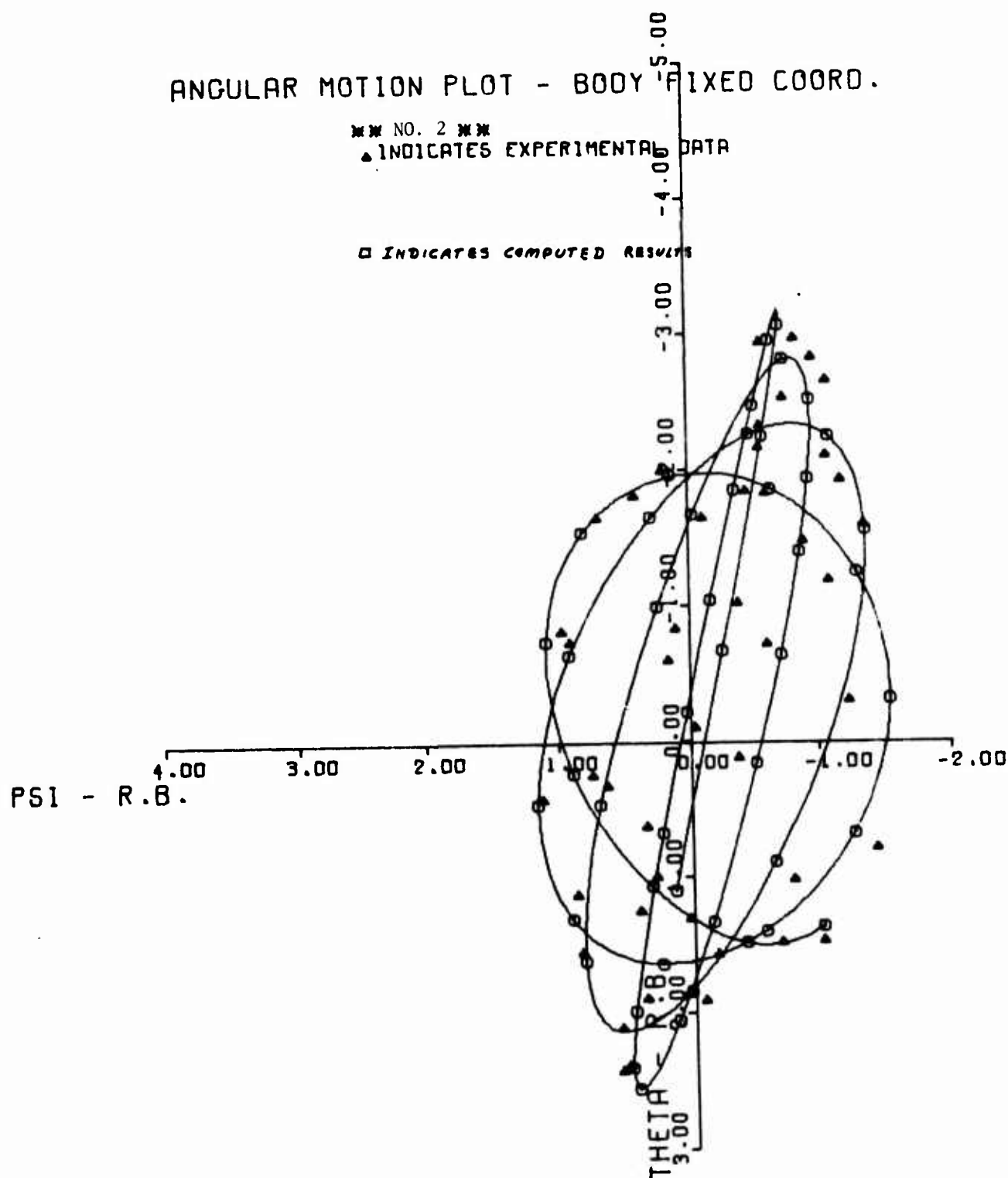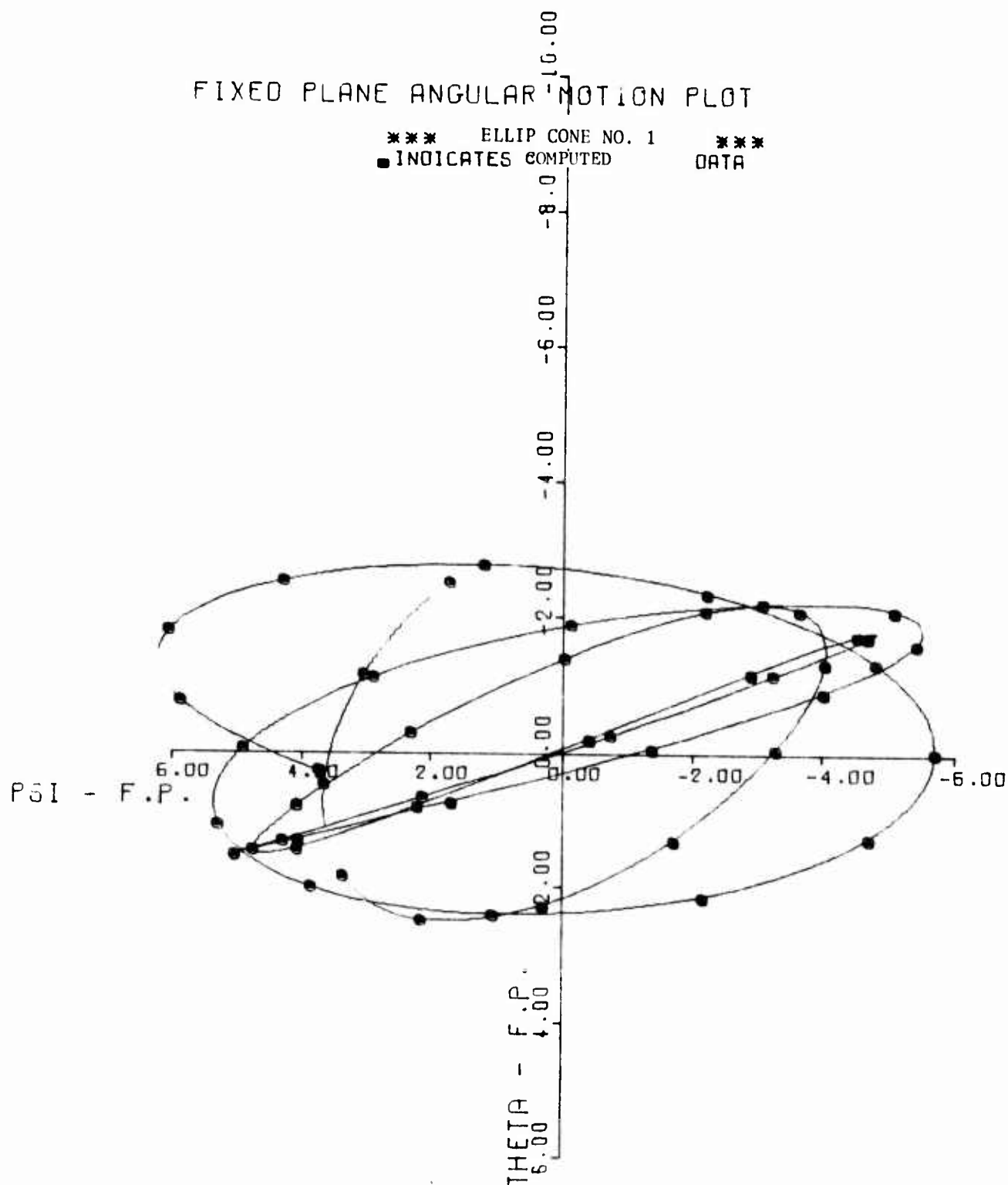
Simultaneous swerve and angular motion reductions were performed utilizing the programs MUL-HEEVE and MANGLES. The result, Table 2, of this final reduction was a better determined set of common aerodynamics with a unique set of trim coefficients for each cone. The spin or roll rate dependent aerodynamic effects (magnus and spin decay) were not computed since the roll rate was very small.

The accuracy of the determined force and moment coefficients must be discussed in terms of their importance towards affecting the observed motion of each cone. The angular motion of Cone No. 1 was about twice the magnitude of Cone No. 2 and contained a roll reversal whereas No. 2 had an increasing roll angle throughout the flight. Intuitively, it should be expected that the correlation of data for Cone No. 1 would result in better determined coefficients for the 2- to 6-degree angle of attack region, and Cone No. 2 for the 0- to 2-degree region. Assuming that both cones represent the same configuration, simultaneous correlation to both sets of observed motion should result in determined aerodynamics covering the 0- to 6-degree angle of attack region.

The computed trim moments (C_{mo}, C_{no}) were of small magnitude, but well determined since they are dominant terms in the equations of motion. They result in trim angles of 0.214 degree for Cone No. 1 and 0.291 degree for Cone No. 2. The pitching moment coefficient derivatives (Cm_α, Cn_β) were well determined and differed by about 28 and 21 percent for Cones 1 and 2 respectively. A roll induced pitching moment term was computed for Cone No. 1. Inclusion of this term into the model being correlated to the data resulted in reducing the probable error of fit to the angular motion data by 10 percent. The induced pitching moment is plotted as a function of aerodynamic roll angle and angle of attack in Figures 10 and 11 respectively. The contribution of the induced effect to the pitching moment is of the order of 3 percent for Cone No. 1. The correlation to the angular motion for Cone No. 2 was not improved by including the induced effect in the reduction. This is probably a result of the smaller angular motion and may, in part, account for the difference in Cn_β between the single reduction fits. Simultaneous analysis of the two cones resulted in a common pitching moment with induced effect included.

The induced roll moment ($C_{\ell\phi}$) was very critical in correlating the roll data since the spin rate was very small. The roll history for Cone No. 1 contains a roll reversal. Figures 12 and 13 illustrate the induced roll moment coefficient plotted as a function of aerodynamic roll angle and angle of attack, respectively.

The damping is probably the most difficult parameter to determine. It is a dynamic term and considering the time period (0.1 second) of the data, its effect on the motion should be relatively small. The damping moment coefficient determined was constrained to be equal in each body-fixed plane. Computation of unique moment components in each plane resulted in no improvement in the correlation to the data.

46
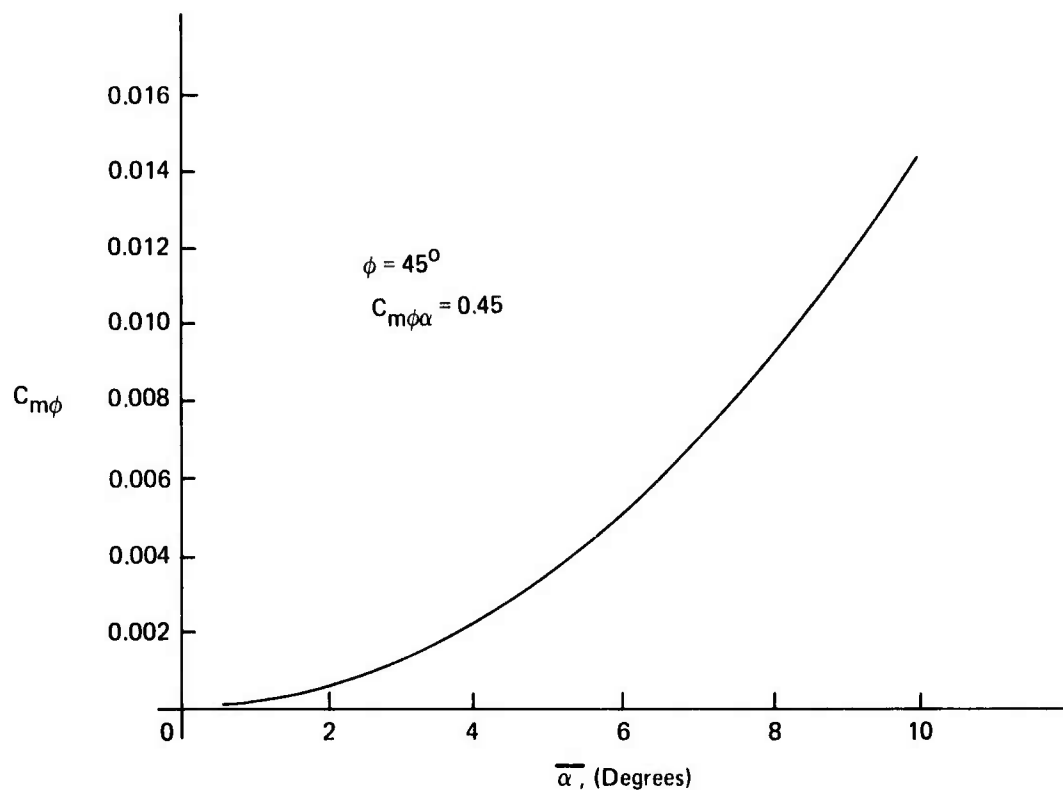
Figure 10. Induced Pitch Moment Coefficient versus $\overline{a}$
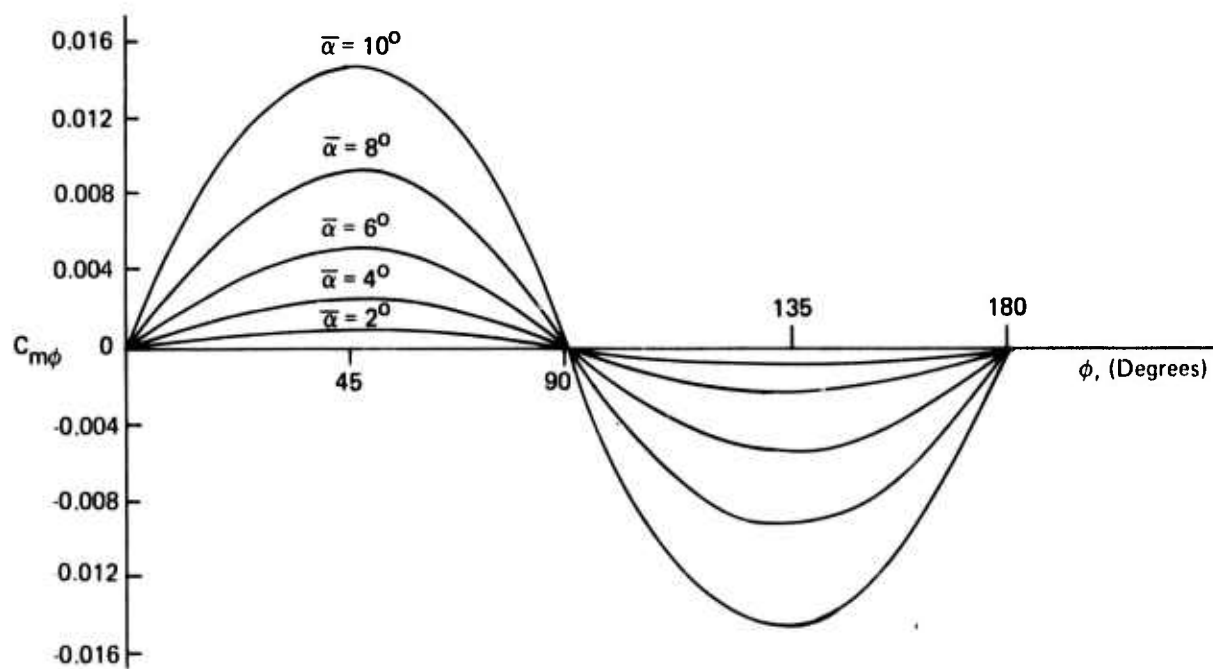
Figure 11. Induced Pitch Moment Coefficient versus ϕ
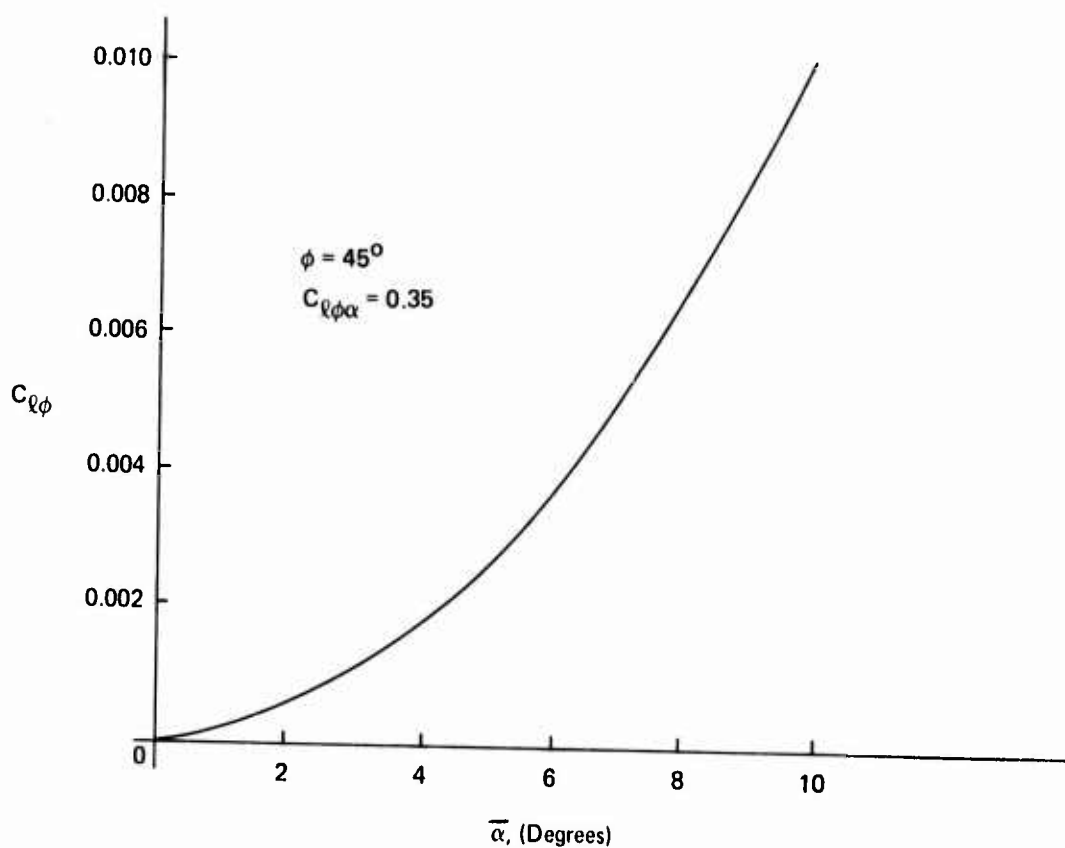
Figure 12. Induced Roll Moment Coefficient versus $\overline{\alpha}$
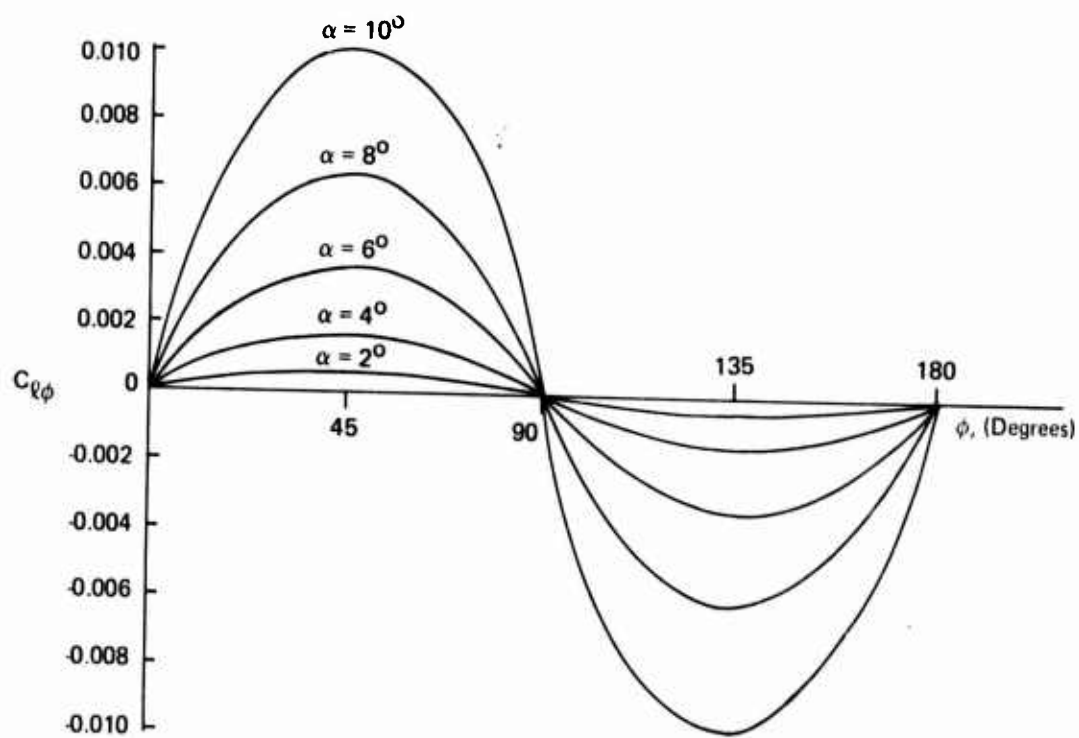
Figure 13. Induced Roll Moment Coefficient versus ϕ

48

Simultaneous analysis of the swerve data resulted in valid axial force and normal force coefficients for the 0- to 6-degree angle of attack region. Table 2 indicates variation in the coefficients determined from individual fits to the data. However, considering the distribution and magnitude of the angular motion data (Figures 7 to 9), the actual forces computed are consistent between the individual and multiple correlations to the data. Cone No. 2 had small angular motion. Therefore, computation of axial force as a function of angle of attack was not meaningful. It is felt that simultaneous analysis provided a good distribution of data to result in an accurate computation of the force coefficients.

SECTION VI

CONCLUSIONS

SUMMARY

A model (equations of motion) has been developed which is capable of computing the six-degree-of-freedom trajectory of a nonsymmetric missile. The derivation of the dynamic equations does not include the effects of the Earth's curvature and rotation. The forces and moments considered to be acting on the missile are described in a body-fixed coordinate system. The inertial frame of reference for the model is the Earth. Aerodynamic coefficients are used to define the forces and moments. They are assumed to be nonlinear functions of the total angle of attack, components of the angle of attack, and the aerodynamic roll angle. Polynomial expansions are made as functions of the sine of the aforementioned angles. Mach number dependencies of the forces and moments have not been included with the exception of the axial force. Modeling of the forces and moments has been done to include a large class of flying objects. The generalized model is suitable for application in the analysis of ballistic spark range data.

Ballistic spark range data provide the actual trajectory. The analysis of that data requires adjusting the aerodynamic coefficients of the equations of motion such that the theoretical trajectory matches the actual. A least squares data correlation technique has been developed which forms the basis of a sensitivity analysis used to adjust the coefficients. A system of sensitivity equations of partial differential equations are developed based on a truncated Taylor's series expansion. These are derived from the six-degree-of-freedom equations of motion. Using the least squares method of correlation, analysis of the translational motion is decoupled from the analysis of the angular motion.

Five computer programs have been developed to result in a data analysis system for correlating ballistic spark range data on a nonsymmetric configuration. The first program of the series (ROLLNUT) correlates the angular motion data to a modified linear theory yaw equation. The primary objective of this program is to compute initial estimates of the linear aerodynamic coefficients and initial conditions, and approximations for the body-fixed angles and angular rates. The second program, ROLL-HEEVE, is used to determine the aerodynamic force coefficients through correlation of the translational data (X, Y, Z) to the earth-fixed equations of motion. Correlation of the angular motion data $(\theta_{RB}, \psi_{RB}, \phi)$ to the body-fixed equations of

50

motion is done next in the sequence using ROLL-ANGLES to determine the aerodynamic moment coefficients. These three programs are capable of computing the optimum set of aerodynamic force and moment coefficients to minimize the probable error of fit to a set of ballistic spark range data. The remaining two programs are used for simultaneous correlation of up to three sets of data on similar configurations to determine a common set of aerodynamic coefficients. The program MUL-HEEVE is used to correlate the translational motion, and MANGLE correlates the angular motion data. The equations of motion and sensitivity equations are numerically integrated using a fourth order Runge-Kutta technique.

Simulated motion was used for preliminary checking of the model and data correlation technique. Ballistic spark range data on two elliptic cones was analyzed using this data analysis system. The resulting probable error of fit was approximately the experimental accuracy of the data. The side force, normal force, pitching moment, yawing moment, and trim forces and moments were determined. A roll induced moment dependent on the aerodynamic roll angle and square of the total angle of attack was also determined. Simultaneous analysis of the two data sets resulted in a well determined set of common aerodynamics for the elliptic cones.

RECOMMENDATIONS

As previously stated, the model represents a large class of flying objects. Therefore, given an actual trajectory, there are many possible combinations of aerodynamic coefficients available to consider in determining those which represent the forces and moments on the missile. Information contained in the system of sensitivity equations could aid in determining which aerodynamic coefficients provide the most accurate representation in matching the actual trajectory. This should be considered in future investigations.

The aerodynamic model derived is felt to be accurate and complete for the analysis of ballistic spark range data on a nonsymmetric configuration. It has been successfully used in the analysis of two elliptic cones. However, it should be noted that there are many possible formulations of the aerodynamic forces and moments. As more experience is gained in analyzing asymmetric configurations, improvements in the manner of modeling the aerodynamics may be desired. These improvements will probably be in the functional relationships of the forces and moments on the angle of attack, angle of attack components, and aerodynamic roll angle.

Least-squares theory has been used as the basis for the sensitivity analysis which represents the data correlation technique. The swerve motion is decoupled from the angular motion resulting in a two-phase data analysis concept. This concept has been very successful in analyzing a large number of data sets on symmetric configurations (Reference 14-22) as well as in analyzing

51

the two elliptic cones on the body-fixed reduction programs. However, the Maximum Likelihood Method is also a suitable data correlation technique. This technique can be used to correlate all six degrees of freedom simultaneously for a determination of the aerodynamic force and moment coefficients. Briefly, this method has the capability of introducing statistical information pertaining to the measurement accuracy into the reduction process (Reference 24). Ballistic spark range data has been analyzed using the Maximum Likelihood Method (Reference 25). It is recommended that consideration be given for utilization of this technique in future investigations towards eliminating the decoupling of the swerve and angular motion analysis.

REFERENCES

1. Mermagen, W.H., "Measurements of the Dynamical Behavior of Projectiles Over Long Flight Paths," Journal of Spacecraft and Rockets, Vol. 8, No. 4, April 1971, pp. 380-385.

2. Murphy, C.H., "Data Reduction for the Free Flight Spark Ranges," BRL Report 900, February 1954.

3. Murphy, C.H., "Free Flight Motion of Symmetric Missiles," BRL Report 1216, July 1963.

4. Murphy, C.H., "The Measurement of Non-Linear Forces and Moments by Means of Free Flight Tests," BRL Report No. 974, February 1956.

5. Krial, K.S. and MacAllister, L.C., "Aerodynamic Properties of a Family of Shell of Similar Shape – 105MM XM380E5, XM380E6, T388 and 155MM T387," BRL MR 2023, February 1970.

6. Nicolaides, J.D. and MacAllister, L.C., "A Review of Aeroballistic Range Research on Winged and/or Finned Missile," Ballistic TN No. 5, Bureau of Ordinance, Dept. of Navy, 1955.

7. Nicolaides, J.D., "Free Flight Dynamics," University of Notre Dame, South Bend, Indiana, 1967.

8. Nicolaides, J.D., "On the Free Flight Motion of Missiles Having Slight Configurational Asymmetries," BRL Report No. 858, June 1953.

9. Nicolaides, J.D., "History of Ordnance Flight Dynamics," AIAA Paper No. 70-533, May 1970.

10. Eikenberry, R.S., "Analysis of the Angular Motion of Missiles," University of Notre Dame, Sandia Report SC-CR-70-6051, February 1970.

11. Chapman, G.T. and Kirk, D.B., "A Method for Extracting Aerodynamic Coefficients from Free Flight Data," AIAA Journal, Vol. 8, No. 4, April 1970.

12. Knadler, C.E., "A Method for Determining the Parameters of Ordinary Differential Equations," NOL TR 68-192, November 1968.

13. Goodman, T.R., "System Identification and Prediction — An Algorithm Using a Newtonian Iteration Procedure," Quarterly of Applied Mathematics, 24 No. 3, 1966, pp. 249-255.

14. Whyte, R.H. and Beliveau, J.G., "An Investigation of the Chapman-Kirk Free Flight Data Reduction Technique", Advance Munitions Report, GE Company, Burlington, Vermont, August 1969.

15. Whyte, R.H. and Beliveau, J.G., "Nonlinear Free Flight Aerodynamic Reduction Using Angle of Attack or Angular Rate Data," General Electric Report TIS R69APB6, September 1969.

16. Whyte, R.H. and Beliveau, J.G., "Reduction of 4.2 Inch Mortar Free Flight Spark Range Data by Numerical Integration," Advance Munitions Report, GE Company, Burlington, Vermont, August 1970.

17. Whyte, R.H. and Hathaway, W.H., "Reduction of Yaw Sonde and Position Time Radar Data by Numerical Integration," General Electric Report 72APB506, January 1972.

18. Whyte, R.H., Jeung, A. and Bradley, J.W., "Chapman-Kirk Reduction of Free Flight Range Data to Obtain Nonlinear Aerodynamic Coefficients," BRL MR 2298, May 1973.

19. Whyte, R.H. and Mermagen, W.H., "A Method for Obtaining Aerodynamic Coefficients from Yaw Sonde and Radar Data," Journal of Spacecraft and Rockets, Vol. 10, No. 6, June 1973, pp. 384-388.

20. Whyte, R.H. and Houghton, R.C., "Reduction of Range and Yaw Sonde Data Using Numerical Integration Techniques," General Electric, Burlington, Vermont, Report No. 72APB539, September 1972.

21. Whyte, R.H., Houghton, R.C. and Hathaway, W.H., "Description of Yaw Sonde Numerical Integration Data Reduction Computer Programs," General Electric, Burlington, Vermont, Report No. 73APB514, May 1973.

22. Whyte, R.H., Hathaway, W.H., "Aeroballistic Range Data Reduction Technique Utilizing Numerical Integration, AFATL-TR-74-41, February 1974.

23. Brunk, J., "User's Manual: Extended Capability Magnus Rotor and Ballistic Body 6-DOF Trajectory Program," AFATL-TR-70-40, May 1970.

24. Grove, R.D., Bowles, R.L. and Mayhew, S.C., "A Procedure for Estimating Stability and Control Parameters from Flight Test Data by Using Maximum Likelihood Methods Employing a Real-Time Digital System," Langley Research Center, NASA TN D-6735, May 1972.

25. Hathaway, W.H., "Analysis of the Free Flight Aerodynamics on Non-Symmetric Bodies from Ballistic Spark Range Data, Thesis, University of Vermont, February 1976.

BIBLIOGRAPHY

1. Barnett, B., "Trajectory Equations for a Six Degree of Freedom Missile Using a Fixed Plane Coordinate System," Picatinny Arsenal Report TR3391, June 1966.

2. Bullock, T., Clarkson, M., Daniel, D., "Preliminary Report on Extracting Aerodynamic Coefficients from Dynamic Data," AFATL-TR-72-52, March 1972.

3. Daniel, D., "An Analysis of Methods for Extracting Aerodynamic Coefficients from Test Data," AFATL-TR-73-32, February 1973.

4. McShane, E.J., Kelley, J.L., Reno, F.V., Exterior Ballistics, University of Denver Press, 1953.

5. Nielson, J.N., "Computer Program for Six Degrees of Freedom Missile Trajectories," Picatinny Arsenal Report TM1292, November 1963.

6. Whyte, R.H., Walker, R. and Hathaway, W.H., "User Manual for AEDC Range G Body Fixed Free Flight Reduction Computer Programs," Advanced Munitions Report, General Electric, Burlington, Vermont, September 1974.

APPENDIX A

EQUATIONS OF MOTION

PARTIAL DERIVATIVES SWERVE ANALYSIS

Derivation of the partial derivatives used in the swerve analysis follows. Parameters computed during analysis of the angular motion are w_{RB}/V, v_{RB}/V, θ_{FP}, ψ_{FP}, and ϕ. These are not treated as dependent variables.

The aerodynamics used in the swerve analysis are defined as follows:

$$\bar{C}_x = C_{x0} + C_{x\alpha 2}\left(\frac{\omega_{RB}}{V}\right)^2 + C_{x\beta 2}\left(\frac{V_{RB}}{V}\right)^2 + C_{xm}\,(M - MREF)$$

$$\bar{C}_Y = C_{y0} + C_{y\beta}\left(\frac{V_{RB}}{V}\right) + C_{y\beta 3}\left(\frac{V_{RB}}{V}\right)^3$$

$$\bar{C}_z = C_{z0} + C_{z\alpha}\left(\frac{\omega_{RB}}{V}\right) + C_{z\alpha 3}\left(\frac{\omega_{RB}}{V}\right)^3$$

$$\bar{C}_{yp} = C_{yp\alpha}\left(\frac{\omega_{RB}}{V}\right)$$

$$\bar{C}_{zp} = C_{zp\beta}\left(\frac{V_{RB}}{V}\right)$$

Consider the $\dot{V}_x$ EOM:

$$\dot{V}_x = \left(\frac{\rho A V^2}{2m}\right)\left[-\bar{C}_x \cos\theta_{FP}\cos\psi_{FP} - \bar{C}_Y\left(\sin\theta_{FP}\cos\psi_{FP}\sin\phi - \sin\psi_{FP}\cos\phi\right)\right.$$

$$- \bar{C}_z\left(\sin\theta_{FP}\cos\psi_{FP}\cos\phi + \sin\psi_{FP}\sin\phi\right)$$

$$+ \bar{C}_{yp}\left(\frac{Pd}{2V}\right)\left(\sin\theta_{FP}\sin\phi\cos\psi_{FP} - \sin\psi_{FP}\cos\phi\right)$$

$$\left.- C_{zp}\left(\frac{Pd}{2V}\right)\left(\sin\theta_{FP}\cos\phi\cos\psi_{FP} + \sin\phi\sin\psi_{FP}\right)\right] \tag{A-1}$$

Taking the partial derivative of $\dot{V}_x$:

$$\frac{\partial \dot{V}_x}{\partial C_j} = A_1 \frac{\partial V}{\partial C_j} + K_{1j} \frac{\partial C_j}{\partial C_j} \qquad \text{(A-2)}$$

where:

$$V = \left[V_x^2 + V_y^2 + V_z^2 \right]^{1/2}$$

$$\frac{\partial V}{\partial C_j} = \frac{V_x}{V} \frac{\partial V_x}{\partial C_j} + \frac{V_y}{V} \frac{\partial V_y}{\partial C_j} + \frac{V_z}{V} \frac{\partial V_z}{\partial C_j}$$

$$A_1 = \left(\frac{\rho A V}{2m}\right) \left[-\left(2C_{xo} + 2C_{x\alpha2}\left(\frac{\omega_{RB}}{V}\right)^2 + 2C_{x\beta2}\left(\frac{V_{RB}}{V}\right)^2 + C_{x\alpha}(3M - 2MREF)\right) \cos\theta_{FP}\cos\psi_{FP}\right.$$

$$- 2\bar{C}_y \left(\sin\theta_{FP}\cos\psi_{FP}\sin\phi - \sin\psi_{FP}\cos\phi\right)$$

$$- 2\bar{C}_z \left(\sin\theta_{FP}\cos\psi_{FP}\cos\phi + \sin\psi_{FP}\sin\phi\right)$$

$$+ \bar{C}_{yp} \left(\frac{Pd}{2V}\right) \left(\sin\theta_{FP}\sin\phi\cos\psi_{FP} - \sin\psi_{FP}\cos\phi\right)$$

$$\left. - \bar{C}_{zp} \left(\frac{Pd}{2V}\right) \left(\sin\theta_{FP}\cos\phi\cos\psi_{FP} + \sin\phi\sin\psi_{FP}\right)\right]$$

$K_{1j} = $ Partial of $\dot{V}_x$ with respect to j^{th} coefficient

e.g. $K_1 = -\left(\frac{\rho A V^2}{2m}\right)\left(\frac{\omega_{RB}}{V}\right)^3 \left(\sin\theta_{FP}\cos\psi_{FP}\cos\phi + \sin\psi_{FP}\sin\phi\right)$

for $C_{z\alpha3}$

Consider the $\dot{V}_y$ EOM:

$$\dot{V}_y = \left(\frac{\rho A V^2}{2m}\right)\left[-\bar{C}_x \cos\theta_{FP}\sin\psi_{FP} - \bar{C}_y \left(\sin\theta_{FP}\sin\psi_{FP}\sin\phi + \cos\psi_{FP}\cos\phi\right)\right.$$

$$- \bar{C}_z \left(\sin\theta_{FP}\sin\psi_{FP}\cos\phi - \cos\psi_{FP}\sin\phi\right)$$

$$+ \bar{C}_{yp} \left(\frac{Pd}{2V}\right) \left(\sin\theta_{FP}\sin\psi_{FP}\sin\phi + \cos\psi_{FP}\cos\phi\right)$$

$$\left. - \bar{C}_{zp} \left(\frac{Pd}{2V}\right) \left(\sin\theta_{FP}\sin\psi_{FP}\cos\phi - \cos\psi_{FP}\sin\phi\right)\right] \qquad \text{(A-3)}$$

Taking the partial derivative of $\dot{V}_y$:

$$\frac{\partial \dot{V}_Y}{\partial c_j} = A_2 \frac{\partial V}{\partial c_j} + K_{2j} \frac{\partial c_j}{\partial c_j} \tag{A-4}$$

where:

$$A_2 = \left(\frac{\rho A V}{2m}\right)\left[-\left(2C_{x_0} + 2C_{x\alpha 2}\left(\frac{\omega_{R3}}{V}\right)^2 + 2C_{x\beta 2}\left(\frac{V_{R0}}{V}\right)^2 + C_{xm}(3M - 2MREF)\right)\cos\theta_{FP}\sin\psi_{FP}\right.$$

$$- 2\bar{C}_y \left(\sin\theta_{FP}\sin\psi_{FP}\sin\phi + \cos\psi_{FP}\cos\phi\right)$$

$$- 2\bar{C}_z \left(\sin\theta_{FP}\sin\psi_{FP}\cos\phi - \cos\psi_{FP}\sin\phi\right)$$

$$+ \bar{C}_{yP}\left(\frac{\rho d}{2V}\right)\left(\sin\theta_{FP}\sin\psi_{FP}\sin\phi + \cos\psi_{FP}\cos\phi\right)$$

$$\left. - \bar{C}_{zP}\left(\frac{\rho d}{2V}\right)\left(\sin\theta_{FP}\sin\psi_{FP}\cos\phi - \cos\psi_{FP}\sin\phi\right)\right]$$

K_{2j} = Partial of $\dot{V}_Y$ with respect to the jth coefficient

Consider the $\dot{V}_z$ EOM:

$$\dot{V}_z = \left(\frac{\rho A V^2}{2m}\right)\left[-\bar{C}_x \sin\theta_{FP} - \bar{C}_y \sin\phi\cos\theta_{FP}\right.$$

$$- \bar{C}_z \cos\phi\cos\theta_{FP} + \bar{C}_{yP}\left(\frac{\rho d}{2V}\right)\sin\phi\cos\theta_{FP}$$

$$\left. - \bar{C}_{zP}\left(\frac{\rho d}{2V}\right)\cos\phi\cos\theta_{FP}\right] - g \tag{A-5}$$

59

Taking the partial of $\dot{V}_z$:

$$\frac{\partial \dot{V}_z}{\partial C_j} = A_3 \frac{\partial V}{\partial C_j} + K_{3j} \frac{\partial C_j}{\partial C_j} \tag{A-6}$$

where:

$$A_3 = \left(\frac{\rho A V}{2m}\right)\left[-\left(2C_{x_0} + 2C_{x_{\alpha 2}}\left(\frac{\omega_{RB}}{V}\right)^2 + 2C_{x_{\beta 2}}\left(\frac{V_{RB}}{V}\right)^2 + C_{xm}(3M - 2M_{REF})\right) \sin\Theta_{FP}\right.$$

$$- 2\bar{C}_y(\sin\phi\cos\Theta_{FP}) - 2\bar{C}_z(\cos\phi\cos\Theta_{FP}) + \bar{C}_{yp}\left(\frac{pd}{2V}\right)(\sin\phi\cos\Theta_{FP})$$

$$\left.- \bar{C}_{zp}\left(\frac{pd}{2V}\right)(\cos\phi\cos\Theta_{FP})\right]$$

Equations A-1, A-3, and A-5 are the equations of motion used to correlate the position data. Equations A-2, A-4, and A-6 are the corresponding partial derivatives. A preliminary analysis of the roll data (ϕ) is done during the swerve analysis. The following equations of motion are used which assume that the product of inertia, I_{xy}, is zero.

$$\dot{P} = \left(\frac{\bar{q} A d}{I_x}\right)\left[\left(\frac{pd}{2V}\right)C_{\ell p} + C_{\ell s} + C_{\ell\phi} \sin^2\bar{\alpha} \sin(n\phi')\right] + \left(\frac{I_y - I_z}{I_x}\right)qr \tag{A-7}$$

$$\dot{\phi} = P + TAN\,\Theta_{FP}\left(q\sin\phi + r\cos\phi\right) \tag{A-8}$$

where:

n = no. of fins or symmetries

ϕ' = aerodynamic roll angle

$= TAN^{-1}\left(\frac{v_{RB}}{w_{RB}}\right)$

60

Taking the partial of $\dot{P}$:

$$\frac{\partial \dot{P}}{\partial c_j} = A_4 \frac{\partial P}{\partial c_j} + K_{4j} \frac{\partial c_j}{\partial c_j} \tag{A-9}$$

where:

$$A_4 = \left(\frac{q\,Ad}{I_x}\right)\left(\frac{d}{2V}\right) C_{\ell p}$$

$$K_{4j} = \text{Partial of P with respect to the j}^{Th} \text{ coefficient}$$

Taking the partial of ϕ:

$$\frac{\partial \dot{\phi}}{\partial c_j} = \frac{\partial P}{\partial c_j} + A_5 \frac{\partial \phi}{\partial c_j} \tag{A-10}$$

where:

$$A_5 = TAN\,\Theta_{FP}\,(q\,cos\phi - r\,sin\phi)$$

ANGULAR MOTION ANALYSIS

Derivation of the partial derivatives used in the angular motion analysis follows. The total velocity is treated as a known based on the swerve analysis.

The aerodynamic forces and moments used in the angular motion analysis are as follows:

$$L_P = \bar{q} A d \left[C_{l_\delta} + \left(\frac{Pd}{2V}\right) C_{l_P} + C_{l\phi} \, SIN^2 \tilde{\alpha} \, SIN(n\phi') \right] \tag{A-11}$$

$$L_q = \bar{q} A d \left[C_{m_o} + C_{m\alpha}\left(\frac{w_{R_B}}{V}\right) + C_{m\alpha_3}\left(\frac{w_{R_B}}{V}\right)^3 + \left(\frac{qd}{2V}\right) C_{m_q} \right.$$

$$+ C_{m_{q_2}} \left(\frac{qd}{2V}\right)\left(\frac{w_{R_B}}{V}\right)^2 + C_{m_{P\beta}}\left(\frac{Pd}{2V}\right)\left(\frac{v_{R_B}}{V}\right) + C_{m\phi\alpha} SIN^2\tilde{\alpha} \, SIN(n\phi')\left(\frac{w_{R_B}}{V}\right)$$

$$\left. + C_{n\phi\alpha} \, SIN^2\tilde{\alpha} \, SIN(n\phi') \left(\frac{v_{R_B}}{V}\right) \right] \tag{A-12}$$

$$L_r = \bar{q} A d \left[C_{n_o} + C_{n\beta}\left(\frac{v_{R_B}}{V}\right) + C_{n\beta_3}\left(\frac{v_{R_B}}{V}\right)^3 + C_{n_r}\left(\frac{rd}{2V}\right)\left(\frac{v_{R_B}}{V}\right) \right.$$

$$+ C_{n_{r_2}}\left(\frac{rd}{2V}\right)\left(\frac{v_{R_B}}{V}\right)^2 + C_{n_{P\alpha}}\left(\frac{Pd}{2V}\right)\left(\frac{w_{R_B}}{V}\right) - C_{m\phi\alpha} \, SIN^2\tilde{\alpha} \, SIN(n\phi')\left(\frac{v_{R_B}}{V}\right)$$

$$\left. + C_{n\phi\alpha} \, SIN^2\tilde{\alpha} \, SIN(n\phi')\left(\frac{w_{R_B}}{V}\right) \right] \tag{A-13}$$

$$F_y = \bar{q} A \left[C_{y_o} + C_{y\beta}\left(\frac{v_{R_B}}{V}\right) + C_{y\beta_3}\left(\frac{v_{R_B}}{V}\right)^3 + C_{y_{P\alpha}}\left(\frac{Pd}{2V}\right)\left(\frac{w_{R_B}}{V}\right) \right] \tag{A-14}$$

$$F_z = \bar{q} A \left[C_{z_o} + C_{z\alpha}\left(\frac{w_{R_B}}{V}\right) + C_{z\alpha_3}\left(\frac{w_{R_B}}{V}\right)^3 + C_{z_{P\beta}}\left(\frac{Pd}{2V}\right)\left(\frac{v_{R_B}}{V}\right) \right] \tag{A-15}$$

Note: The induced normal and side forces indicated by Equations (39a) and (39e) are not included in the programs.

For convenience of derivation, the following identities will be stated:

$$SIN^2 \, \bar{\alpha} = \frac{V_{RB}^2 + W_{RB}^2}{V^2}$$

$$SIN(n\phi') = SIN\left(n \, TAN^{-1}\left(\frac{V_{RB}}{W_{RB}}\right)\right)$$

$$PFINV = \frac{\partial \, SIN(n\phi')}{\partial \, V_{RB}} = COS(n\phi')\left[\frac{W_{RB}}{V_{RB}^2 + W_{RB}^2}\right]$$

$$PFINW = \frac{\partial \, SIN(n\phi')}{\partial \, W_{RB}} = -COS(n\phi')\left[\frac{V_{RB}}{V_{RB}^2 + W_{RB}^2}\right]$$

$$PSFSAV = \frac{\partial \, SIN^2\bar{\alpha} \, SIN(n\phi')}{\partial \, V_{RB}} = SIN^2\bar{\alpha} \, (PFINV) + SIN(n\phi')\left(\frac{2V_{RB}}{V^2}\right)$$

$$PSFSAW = \frac{\partial \, SIN^2\bar{\alpha} \, SIN(n\phi')}{\partial \, W_{RB}} = SIN^2\bar{\alpha} \, (PFINW) + SIN(n\phi')\left(\frac{2W_{RB}}{V^2}\right)$$

$$PINDVV = \frac{\partial \left[SIN^2\bar{\alpha} \, SIN(n\phi')\left(\frac{V_{RB}}{V}\right)\right]}{\partial \, V_{RB}} = PSFSAV\left(\frac{V_{RB}}{V}\right) + SIN^2\bar{\alpha} \, SIN(n\phi')\left(\frac{1}{V}\right)$$

$$PINDWW = \frac{\partial \left[SIN^2\bar{\alpha} \, SIN(n\phi')\left(\frac{W_{RB}}{V}\right)\right]}{\partial \, W_{RB}} = PSFSAW\left(\frac{W_{RB}}{V}\right) + SIN^2\bar{\alpha} \, SIN(n\phi')\left(\frac{1}{V}\right)$$

$$IS1 = (I_x + I_y - I_z) \, I_{xy}$$

$$IS2 = (I_{xy}^2 + I_y(I_y - I_z))$$

$$IS3 = (I_x I_y - I_{xy}^2)$$

$$IS4 = (I_x(I_z - I_x) - I_{xy}^2)$$

$$IS5 = (I_x - I_y)$$

The dependent variables to be considered in taking partial derivatives are p, q, r, θ_{FP}, ϕ, v_{RB}, and w_{RB}. Derivation of the partials follows.

Consider the $\dot{P}$ EOM:

$$\dot{P} = \frac{I_y L_p + I_{xy} L_q - (IS1)\, Pr + (IS2)\, qr}{IS3} \tag{A-16}$$

Taking the generalized partial of $\dot{P}$:

$$\frac{\partial \dot{P}}{\partial c_j} = B_1 \frac{\partial P}{\partial c_j} + B_2 \frac{\partial q}{\partial c_j} + B_3 \frac{\partial r}{\partial c_j} + B_4 \frac{\partial V_{RB}}{\partial c_j} + B_5 \frac{\partial w_{RB}}{\partial c_j} + K_{5j} \frac{\partial c_j}{\partial c_j} \tag{A-17}$$

where:

$$B_1 = -\frac{IS1}{IS3}\, r + \frac{I_y}{IS3} \frac{\partial L_p}{\partial P} + \frac{I_{xy}}{IS3} \frac{\partial L_q}{\partial P}$$

$$B_2 = \frac{IS2}{IS3}\, r + \frac{I_{xy}}{IS3} \frac{\partial L_q}{\partial q}$$

$$B_3 = \frac{IS2}{IS3}\, q - \frac{IS1}{IS3}\, P$$

$$B_4 = \frac{I_x}{IS3} \frac{\partial L_p}{\partial V_{RB}} + \frac{I_{xy}}{IS3} \frac{\partial L_q}{\partial V_{RB}}$$

$$B_5 = \frac{I_x}{IS3} \frac{\partial L_p}{\partial w_{RB}} + \frac{I_{xy}}{IS3} \frac{\partial L_q}{\partial w_{RB}}$$

K_{5j} = Partial of $\dot{P}$ with respect to the j^{Th} coefficient

Consider the $\dot{q}$ EOM:

$$\dot{q} = \frac{I_x L_q + I_{xy} L_p + (IS1)qr + (IS4)Pr}{IS3} \tag{A-18}$$

Taking the generalized partial of $\dot{q}$:

$$\frac{\partial \dot{q}}{\partial c_j} = D_1 \frac{\partial P}{\partial c_j} + D_2 \frac{\partial q}{\partial c_j} + D_3 \frac{\partial r}{\partial c_j} + D_4 \frac{\partial V_{RB}}{\partial c_j} + D_5 \frac{\partial \omega_{RB}}{\partial c_j} + K_{6j} \frac{\partial c_j}{\partial c_j} \tag{A-19}$$

where:

$$D_1 = \frac{(IS4)}{IS3} r + \frac{I_x}{IS3} \frac{\partial L_q}{\partial P} + \frac{I_{xy}}{IS3} \frac{\partial L_p}{\partial P}$$

$$D_2 = \frac{(IS1)}{IS3} r + \frac{I_x}{IS3} \frac{\partial L_q}{\partial q}$$

$$D_3 = \frac{(IS1)}{IS3} q + \frac{(IS4)}{IS3} P$$

$$D_4 = \frac{I_x}{IS3} \frac{\partial L_q}{\partial V_{RB}} + \frac{I_{xy}}{IS3} \frac{\partial L_p}{\partial V_{RB}}$$

$$D_5 = \frac{I_x}{IS3} \frac{\partial L_q}{\partial \omega_{RB}} + \frac{I_{xy}}{IS3} \frac{\partial L_p}{\partial \omega_{RB}}$$

K_{6j} = Partial of $\dot{q}$ with respect to the j Th coefficient

65

Consider the $\dot{r}$ EOM:

$$\dot{r} = \frac{L_r + I_{xy}(p^2 - q^2) + (ISS)pq}{I_z} \tag{A-20}$$

Taking the generalized partial of $\dot{r}$:

$$\frac{\partial \dot{r}}{\partial c_j} = E_1 \frac{\partial p}{\partial c_j} + E_2 \frac{\partial q}{\partial c_j} + E_3 \frac{\partial r}{\partial c_j} + E_4 \frac{\partial V_{RB}}{\partial c_j} + E_5 \frac{\partial \omega_{RB}}{\partial c_j} + K_{7i} \frac{\partial c_j}{\partial c_j} \tag{A-21}$$

where:

$$E_1 = \frac{2 I_{xy} p}{I_z} + \frac{(ISS)}{I_z} q + \frac{1}{I_z} \frac{\partial L_r}{\partial p}$$

$$E_2 = \frac{(ISS)}{I_z} p - \frac{2 I_{xy}}{I_z} q$$

$$E_3 = \frac{1}{I_z} \frac{\partial L_r}{\partial r}$$

$$E_4 = \frac{1}{I_z} \frac{\partial L_r}{\partial V_{RB}}$$

$$E_5 = \frac{1}{I_z} \frac{\partial L_r}{\partial \omega_{RB}}$$

K_{7j} = Partial of $\dot{r}$ with respect to the j^{Th} coefficient

66

Consider the $\dot{v}_{RB}$ EOM:

$$\dot{V}_{RB} = P w_{RB} - r u_{RB} + F_Y/m - g \sin\phi \cos\Theta_{FP} \tag{A-22}$$

Taking the generalized partial of $\dot{v}_{RB}$:

$$\frac{\partial \dot{V}_{RB}}{\partial C_j} = F_1 \frac{\partial P}{\partial C_j} + F_2 \frac{\partial r}{\partial C_j} + F_3 \frac{\partial V_{PB}}{\partial C_j} + F_4 \frac{\partial w_{RB}}{\partial C_j} + F_5 \frac{\partial \Theta_{FP}}{\partial C_j} + F_6 \frac{\partial \phi}{\partial C_j} \tag{A-23}$$

where:

$$F_1 = w_{RB} + \frac{1}{m} \frac{\partial F_Y}{\partial P}$$

$$F_2 = -u_{RB}$$

$$F_3 = \frac{1}{m} \frac{\partial F_Y}{\partial V_{RB}}$$

$$F_4 = P + \frac{1}{m} \frac{\partial F_Y}{\partial w_{RB}}$$

$$F_5 = g \sin\phi \sin\Theta_{FP}$$

$$F_6 = -g \cos\phi \cos\Theta_{FP}$$

Note: The K_j term does not appear since only the aerodynamic forces appear in the $\dot{v}_{RB}$ and $\dot{w}_{RB}$ equations of motion. These coefficients are not being determined by the angular motion program.

67

Consider the $\dot{w}_{RB}$ EOM:

$$\dot{w}_{RB} = q\,\mu_{RB} - P\,V_{RB} + F_z/m - g\cos\phi\cos\theta_{FP} \tag{A-24}$$

Taking the generalized partial of $\dot{w}_{RB}$:

$$\frac{\partial \dot{w}_{RB}}{\partial c_j} = G_1\frac{\partial P}{\partial c_j} + G_2\frac{\partial q}{\partial c_j} + G_3\frac{\partial r}{\partial c_j} + G_4\frac{\partial w_{RB}}{\partial c_j} + G_5\frac{\partial \theta_{FP}}{\partial c_j} + G_6\frac{\partial \phi}{\partial c_j} \tag{A-25}$$

where:

$$G_1 = -V_{RB} + \frac{1}{m}\frac{\partial F_z}{\partial P}$$

$$G_2 = \mu_{RB}$$

$$G_3 = -P + \frac{1}{m}\frac{\partial F_z}{\partial V_{RB}}$$

$$G_4 = \frac{1}{m}\frac{\partial F_z}{\partial w_{RB}}$$

$$G_5 = g\cos\phi\sin\theta_{FP}$$

$$G_6 = g\sin\phi\cos\theta_{FP}$$

68

Consider the $\dot{\phi}$ EOM:

$$\dot{\phi} = P + TAN\Theta_{FP}(q\,SIN\phi + r\,COS\phi) \qquad (A\text{-}26)$$

Taking the generalized partial of $\dot{\phi}$:

$$\frac{\partial\dot{\phi}}{\partial c_j} = H_1 \frac{\partial P}{\partial c_j} + H_2 \frac{\partial q}{\partial c_j} + H_3 \frac{\partial r}{\partial c_j} + H_4 \frac{\partial\Theta_{FP}}{\partial c_j} + H_5 \frac{\partial\phi}{\partial c_j} \qquad (A\text{-}27)$$

where:

$$H_1 = 1.0$$

$$H_2 = TAN\,\Theta_{FP}\,SIN\phi$$

$$H_3 = TAN\,\Theta_{FP}\,COS\phi$$

$$H_4 = SEC^2\Theta_{FP}\,(q\,SIN\phi + r\,COS\phi)$$

$$H_5 = TAN\Theta_{FP}\,(q\,COS\phi - r\,SIN\phi)$$

Consider the $\dot{\theta}$ EOM:

$$\dot{\theta} = q\,COS\phi - r\,SIN\phi \qquad (A\text{-}28)$$

Taking the generalized partial of $\dot{\theta}$:

$$\frac{\partial\dot{\theta}}{\partial c_j} = COS\phi\,\frac{\partial q}{\partial c_j} - SIN\phi\,\frac{\partial r}{\partial c_j} - (q\,SIN\phi + r\,COS\phi)\frac{\partial\phi}{\partial c_j} \qquad (A\text{-}29)$$

69

Taking partial derivatives of Equations (A-11) through (A-15) results in the following:

$$\frac{\partial L_p}{\partial P} = \bar{q} A d \left(\frac{d}{2V}\right) C_{\ell P}$$

$$\frac{\partial L_p}{\partial V_{RB}} = \bar{q} A d\, C_{\ell \phi}\, (PSFSAV)$$

$$\frac{\partial L_p}{\partial u_{RB}} = \bar{q} A d\, C_{\ell \phi}\, (PSFSAW)$$

$$\frac{\partial L_q}{\partial P} = \bar{q} A d \left(\frac{d}{2V}\right) C_{mPB} \left(\frac{V_{RB}}{V}\right)$$

$$\frac{\partial L_q}{\partial q} = \bar{q} A d \left(\frac{d}{2V}\right) \left(C_{mq} + C_{mq2}\left(\frac{w_{RB}}{V}\right)^2\right)$$

$$\frac{\partial L_q}{\partial V_{RB}} = \bar{q} A d \left[\left(\frac{Pd}{2V}\right) C_{mP\beta}\left(\frac{1}{V}\right) + C_{m\phi\alpha}\left(\frac{w_{RB}}{V}\right)(PSFSAV) + C_{n\xi\alpha}\,(PINDVV)\right]$$

$$\frac{\partial L_q}{\partial w_{RB}} = \bar{q} A d \left[C_{m\alpha}\left(\frac{1}{V}\right) + C_{m\alpha3}\left(\frac{3 w_{RB}^2}{V^3}\right) + C_{mq2}\left(\frac{qd}{2V}\right)\left(\frac{2 w_{RB}}{V^2}\right)\right.$$
$$\left. + C_{m\phi\alpha}\,(PINDWW) + C_{n\xi\alpha}\left(\frac{V_{RB}}{V}\right)(PSFSAW)\right]$$

$$\frac{\partial L_r}{\partial P} = \bar{q} A d \left(\frac{d}{2V}\right) C_{nP\alpha} \left(\frac{w_{RB}}{V}\right)$$

$$\frac{\partial L_r}{\partial r} = \bar{q} A d \left(\frac{d}{2V}\right) \left(C_{nr} + C_{nr2}\left(\frac{V_{RB}}{V}\right)^2\right)$$

$$\frac{\partial L_r}{\partial V_{RB}} = \bar{q} A d \left[C_{n\beta}\left(\frac{1}{V}\right) + C_{n\beta3}\left(\frac{3 V_{RB}^2}{V^3}\right) + C_{nr2}\left(\frac{rd}{2V}\right)\left(\frac{2 V_{RB}}{V^2}\right)\right.$$
$$\left. - C_{m\phi\alpha}\,(PINDVV) + C_{n\phi\alpha}\left(\frac{w_{RB}}{V}\right)(PSFSAV)\right]$$

$$\frac{\partial L_r}{\partial w_{RB}} = \bar{q} A d \left[\left(\frac{Pd}{2V}\right) C_{nP\alpha}\left(\frac{1}{V}\right) - C_{m\phi\alpha}\left(\frac{V_{RB}}{V}\right)(PSFSAW)\right.$$
$$\left. + C_{n\xi\alpha}\,(PINDWW)\right]$$

$$\frac{\partial F_Y}{\partial P} = \bar{q}A\left(\frac{d}{2V}\right)C_{YP\alpha}\left(\frac{\omega_{RB}}{V}\right)$$

$$\frac{\partial F_Y}{\partial V_{RB}} = \bar{q}A\left[C_{Y\beta}\left(\frac{1}{V}\right) + C_{Y\beta3}\left(\frac{3V_{RB}^2}{V^3}\right)\right]$$

$$\frac{\partial F_Y}{\partial \omega_{RB}} = \bar{q}A\left[C_{YP\alpha}\left(\frac{Pd}{2V}\right)\left(\frac{1}{V}\right)\right]$$

$$\frac{\partial F_z}{\partial P} = \bar{q}A\left(\frac{d}{2V}\right)C_{ZP\beta}\left(\frac{V_{RB}}{V}\right)$$

$$\frac{\partial F_z}{\partial V_{RB}} = \bar{q}A\left(\frac{Pd}{2V}\right)C_{ZP\beta}\left(\frac{1}{V}\right)$$

$$\frac{\partial F_z}{\partial \omega_{RB}} = \bar{q}Ad\left[C_{Z\alpha}\left(\frac{1}{V}\right) + C_{Z\alpha3}\left(\frac{3\omega_{RB}^2}{V^3}\right)\right]$$

APPENDIX B

COMPUTER PROGRAM INPUT INSTRUCTIONS

CARD NO. 1 (10A3)

IBM Col	Variable	Descriptor
1-30	SHOTN	Title Card

CARD NO. 2 (7I7)

1-7	LN	Start point of fit
8-14	NA	End point of fit
15-21	ND	Incremental section length
22-28	NAUTO	0 input ω_1, ω_2 1 input CMAE
29-35	NROLL	0 roll data on card No. 3 2 roll data on card No. 5
36-42	NCOORD	0 AEDC data 1 Eglin or test case data
43-49	NBODY	0 Output in fixed plane 1 Output in body axis

Normal Settings -	Eglin	AEDC
NAUTO	0	0
NROLL	0	2
NCOORD	1	0
NBODY	1	1

CARD NO. 3a,z (7F10.0)

1-10	TG	Time, seconds
11-20	XG	X_{range}, inches
21-30	YG	Y_{range}, inches
31-40	ZG	Z_{range}, feet

CARD NO. 3a,z (7F10.0) (continued)

41-50	DMG	m	
			direction
51-60	DNG	n	cosines
61-70	DPE	p	or $\emptyset_{FP}$ (see NROLL)

CARD NO. 4 (1F10.0)

1-10	TG	TG = 200 (stop card)

Note: Card No's 5 and 6 are not supplied when NROLL = 0.

CARD NO. 5 (2E14.6, 1F14.0)

1-14	PHI	$\emptyset_{FP}$
15-28	DUMMY	Z_g – not used
29-42	DUMMI	

CARD NO. 6 (2E14.6, 1F14.0)

1-14	PHI	
15-28	DUMMY	
29-42	DUMMI	DUMMI = 200 (stop card)

CARD NO. 7 (7F10.0)

1-10	DIA	diameter, inches
11-20	AIX	I_x, lb in^2
21-30	AIY	I_y, lb in^2
31-40	AIZ	I_z, lb in^2
41-50	AIXY	I_{xy}
51-60	WGT	weight, lbs.
61-70	ACG	CG offset, inches

CARD NO. 8 (4F10.0)

1-10	XCGR	Reference CG, percent of length
11-20	XLR	Reference length, inches
21-30	XCG	CG, percent of length
31-40	XFIN	No. of assymetries or fins

CARD NO. 9 (3F10.0)

1-10	RHO	density, slugs/ft^3
11-20	ASOUND	speed of sound, ft/sec
21-30	VMACH	reference mach no.

CARD NO. 10 (4F10.0)

1-10	CNA	C_{N_α} estimated
11-20	CMAE	C_{M_α} estimated
21-30	CP	C_{1_p} estimated
31-40	CLD	C_{1_δ} estimated

CARD NO. 11 (6F10.0)

1-10	CA	linear theory
11-20	CB	roll constants
21-30	CC	
31-40	CD	
41-50	XXREF	
51-60	CNOT	

let $X = (X_i - XXREF)$

$$PHI = CA(X) + CB(X^2) + CC(X^3) + CD(X^4) + CNOT$$

<u>CARD NO. 12 (7F10.0)</u>

1-10	B(1)	K_1
11-20	B(2)	K_2
21-30	B(3)	λ_1
31-40	B(4)	λ_2
41-50	B(5)	$\emptyset_1$
51-60	B(6)	$\emptyset_2$
61-70	B(7)	ω_1

<u>CARD NO. 13 (5F10.0)</u>

1-10	B(8)	ω_2
11-20	B(9)	$\dot{\omega}_1$
21-30	B(10)	$\dot{\omega}_2$
31-40	B(11)	K_3
41-50	B(12)	ϕ_3

<u>CARD NO. 14 (13I1)</u>

NCON(J), J = 1,12,NEWST

CCON(J) = NCON(J)   J = 1,12

corresponds to card numbers 12 and 13

NEWST = 0   program will restart with

NCON(11) and NCON(12) equal to 1

NEWST = 1   no restarts allowed

<u>CARD NO. 15 (30I1)</u>

NNCON(J)   J = 1,30 for ROLL-HEEVE

77

CARD NO. 1 (10A3)

IBM Col

| 1-30 | SHOTN | Title |

CARD NO. 2 (8F10.0)

1-10	DPT	Time Step
11-20	RHO	Density
21-30	AS	Speed of Sound
31-40	AMREF	Reference Mach No.

CARD NO. 3 (8F10.0)

1-10	D1	Reference diameter, inches
11-20	AIX	Axial Moment of Inertia, $lb\text{-}in^2$
21-30	AIY	Y-Transverse Moment of Inertia, $lb\text{-}in^2$
31-40	AIZ	Z-Transverse Moment of Inertia, $lb\text{-}in^2$
41-50	AIXY	Product of Inertia
51-60	WGT	Weight, lbs.
61-70	ACG	Offset CG

CARD NO. 4 (8F10.0)

1-10	XCGR	Reference CG, percent of length
11-20	XLR	Reference length, inches
21-30	XCG	CG, percent of length
31-40	XFIN	No of Fins or Assymetries

CARD NO. 5 (8F10.0)

1-10	TCON(1)	θ_{RB_o}, degrees
11-20	TCON(2)	q_o, deg/sec
21-30	TCON(3)	Ψ_{RB_o}, degrees
31-40	TCON(4)	r_o, deg/sec
41-50	TCON(5)	$C_{m\alpha}$ —
51-60	TCON(6)	C_{mq} —
61-70	TCON(7)	$C_{np\alpha}$ —
71-80	TCON(8)	Not used

CARD NO. $6_{(1)}$ to $6_{(NT)}$ (8F10.0)   Experimental Data

1-10	TIME(K)	Time, sec
11-20	DIST(1,K)	X Distance, ft
21-30	DIST(2,K)	Y Distance, ft
31-40	DIST(3,K)	Z Distance, ft
41-50	PHIX(K)	$\emptyset$, radians
51-60	THETFP(K)	θ_{FP}, degrees
61-70	PSIFP(K)	Ψ_{FP}, degrees

CARD NO. $6_{(NT+1)}$

1-10	200.	Stop Card

CARD NO. $7_{(K)}$ to $7_{(NNN)}$ (8F10.0)   From ROLL-NUT

1-10	XTIME(K)	Time, seconds
11-20	XQ(K)	Q, deg/ft

CARD NO. 7$_{(K)}$ to 7$_{(NNN)}$ (8F10.0)   (continued)

21-30	XR(K)	R, deg/ft
31-40	TRB	θ_{RB}, degrees
41-50	PRB	Ψ_{RB}, degrees
51-60	XPHI(K)	$\emptyset_C$, radians

CARD NO. 7$_{(NNN+1)}$

1-10	200.	Stop Card

CARD NO. 8 (8F10.0)

1-10	ACON(1)	X_o, feet
11-20	ACON(2)	$\dot{X}_o$, ft/sec
21-30	ACON(3)	Y_o, feet
31-40	ACON(4)	$\dot{Y}_o$, ft/sec
41-50	ACON(5)	Z_o, feet
51-60	ACON(6)	$\dot{Z}_o$, ft/sec
61-70	ACON(7)	C_{X_o}
71-80	ACON(8)	$C_{X\alpha_2}$

CARD NO. 9 (8F10.0)

1-10	ACON(9)	$C_{X\beta_2}$
11-20	ACON(10)	C_{X_m}
21-30	ACON(11)	C_{Y_o}
31-40	ACON(12)	$C_{Y\beta}$
41-50	ACON(13)	$C_{Y\beta_3}$
51-60	ACON(14)	C_{N_o}
61-70	ACON(15)	$C_{N\alpha}$
71-80	ACON(16)	$C_{N\alpha_3}$

CARD NO. 10 (8F10.0)

1-10	ACON(17)	$C_{Yp\alpha}$
11-20	ACON(18)	$C_{Yp\beta}$
21-30	ACON(19)	$C_{X\bar{\alpha}_2}$
31-40	ACON(20)	$C_{N\bar{\alpha}}$
41-50	ACON(21)	$C_{N\bar{\alpha}_3}$
51-60	ACON(22)	$C_{Yp\bar{\alpha}}$
61-70	ACON(23)	Not Used
71-80	ACON(24)	P_o, rad/sec

CARD NO. 11 (8F10.0)

1-10	ACON(25)	ϕ_o, radians
11-20	ACON(26)	C_{1p}
21-30	ACON(27)	$C_{1\delta}$
31-40	ACON(28)	$C_{1\phi}$
41-50	ACON(29)	SPNFORM $\left(\text{on } \dfrac{I_y - I_z}{I_x}\right)$
51-60	ACON(30)	Not Used

CARD NO. 12 (30I1)

| 1-30 | NNCON(1) - NNCON(30) | |

ROLL-ANGLE INPUT

CARD NO. 1 (10A3)

| 1-30 | SHOTN | Title |

CARD NO. 2 (10I3)

1-3	LN	Starting Pt. of fit
4-6	NA	End Pt. of Sectional fit
7-9	ND	Incremental section interval
10-12	NB	Summing section interval

CARD NO. 3 (8F10.0)

1-10	DPT	Time step
11-20	RHO	Density
21-30	AS	Speed of sound
31-40	AMREF	Reference Mach No.

CARD NO. 4 (8F10.0)

1-10	D1	Reference diameter, inches
11-20	AIX	Axial Moment of Inertia
21-30	AIY	Y-Transverse Moment of Inertia
31-40	AIZ	Z-Transverse Moment of Inertia
41-50	AIXY	Product of Inertia
51-60	WGT	Weight, lbs.
61-70	ACG	Offset CG

CARD NO. 5 (8F10.0)

1-10	XCGR	Reference CG, percent of length
11-20	XLR	Reference length, inches
21-30	XCG	CG, percent of length
31-40	XFIN	No of Fins or Assymetries

CARD NO. 6 (8F10.0)

1-10	TCON(1)	θ_{RB_o}, degrees
11-20	TCON(2)	q_o, deg/sec
21-30	TCON(3)	Ψ_{RB_o}, degrees
31-40	TCON(4)	r_o, deg/sec
41-50	TCON(5)	$C_{m\alpha}$
51-60	TCON(6)	C_{mq}
61-70	TCON(7)	$C_{np\alpha}$
71-80	TCON(8)	Not used

CARD NO. $7_{(1)}$ to $7_{(NT)}$ (8F10.0)

1-10	TIME(K)	Time, sec
11-20	DIST(1,K)	X Distance, ft
21-30	DIST(2,K)	Y Distance, ft
31-40	DIST(3,K)	Z Distance, ft
41-50	PHIX(K)	$\emptyset$, radians
51-60	THETFP(K)	θ_{FP}, degrees
61-70	PSIFP(K)	Ψ_{FP}, degrees

CARD NO. $7_{(NT+1)}$

1-10	200.	Stop Card

CARD NO. 8 (8F10.0)

1-10	HCON(1)	X_o, feet
11-20	HCON(2)	$\dot{X}_o$, feet/sec
21-30	HCON(3)	Y_o, feet
31-40	HCON(4)	$\dot{Y}_o$, feet/sec

CARD NO. 8 (contd.) (8F10.0)

41-50	HCON(5)	z_o, feet
51-60	HCON(6)	$\dot{z}_o$, feet/sec
61-70	HCON(7)	C_{X_o}
71-80	HCON(8)	$C_{X\alpha_2}$

CARD NO. 9 (8F10.0)

1-10	HCON(9)	$C_{X\beta_2}$
11-20	HCON(10)	C_{X_m}
21-30	HCON(11)	C_{Y_o}
31-40	HCON(12)	$C_{Y\beta}$
41-50	HCON(13)	$C_{Y\beta_3}$
51-60	HCON(14)	C_{N_o}
61-70	HCON(15)	$C_{N\alpha}$
71-80	HCON(16)	$C_{N\alpha_3}$

CARD NO. 10 (8F10.0)

1-10	HCON(17)	$C_{Yp\alpha}$
11-20	HCON(18)	$C_{Yp\beta}$
21-30	HCON(19)	$C_{X\bar{\alpha}_2}$
31-40	HCON(20)	$C_{N\bar{\alpha}}$
41-50	HCON(21)	$C_{N\bar{\alpha}_3}$
51-60	HCON(22)	$C_{Yp\bar{\alpha}}$
61-70	HCON(23)	Not Used
71-80	HCON(24)	p_o, rad/sec

CARD NO. 11 (8F10.0)

1-10	HCON(25)	$\emptyset_o$, radians
11-20	HCON(26)	C_{1p}
21-30	HCON(27)	$C_{1\delta}$
31-40	HCON(28)	$C_{1\emptyset}$
41-50	HCON(29)	SPNFORM $\left(\text{on } \dfrac{I_y - I_z}{I_x}\right)$
51-60	HCON(30)	Not used

CARD NO. 12 (30I1)

1-30	NHCON(1) - NHCON(30)

CARD NO. $13_{(1)}$ to $13_{(NT)}$ (8F10.0)

1-10	TIME(K)	Time, sec
11-20	VEL(K)	Total Velocity, ft/sec
21-30	AQBAR(K)	Dynamic Pressure
31-40	TRB(K)	θ_{RB}, degrees
41-50	PRB(K)	Ψ_{RB}, degrees

CARD NO. $13_{(NT+1)}$

1-10	200.	Stop Card

CARD NO. 14 (8F10.0)

1-10	ACON(1)	θ_{RB_o}, degrees
11-20	ACON(2)	q_o, deg/sec
21-30	ACON(3)	Ψ_{RB_o}, degrees
31-40	ACON(4)	r_o, deg/sec

85

CARD NO. 14 (cont.) (8F10.0)

41-50	ACON(5)	C_{mo}
51-60	ACON(6)	$C_{m\alpha}$
61-70	ACON(7)	$C_{m\alpha_3}$
71-80	ACON(8)	C_{no}

CARD NO. 15 (8F10.0)

1-10	ACON(9)	$C_{n\beta}$
11-20	ACON(10)	$C_{n\beta_3}$
21-30	ACON(11)	C_{mq}
31-40	ACON(12)	C_{mq_2}
41-50	ACON(13)	C_{nr}
51-60	ACON(14)	C_{nr_2}
61-70	ACON(15)	$C_{np\alpha}$
71-80	ACON(16)	$C_{mp\beta}$

CARD NO. 16 (8F10.0)

1-10	ACON(17)	$C_{n\phi\bar{\alpha}}$
11-20	ACON(18)	AIXY
21-30	ACON(19)	AIX
31-40	ACON(20)	$C_{m\phi\bar{\alpha}}$
41-50	ACON(21)	$C_{m\alpha_2}$
51-60	ACON(22)	$C_{n\alpha_2}$
61-70	ACON(23)	$C_{mo\phi}$
71-80	ACON(24)	$C_{no\phi}$

CARD NO. 17 (8F10.0)

1-10	ACON(25)	Not used
11-20	ACON(26)	$C_{m\alpha}$
21-30	ACON(27)	$C_{m\alpha_3}$
31-40	ACON(28)	C_{mq}
41-50	ACON(29)	C_{mq_2}
51-60	ACON(30)	$C_{np\alpha}$
61-70	ACON(31)	Not used
71-80	ACON(32)	Not used

CARD NO. 18 (8F10.0)

1-10	ACON(33)	Not used
11-20	ACON(34)	Not used
21-30	ACON(35)	Not used
31-40	ACON(36)	ϕ_o, radians
41-50	ACON(37)	P_o, rad/sec
51-60	ACON(38)	C_{lp}
61-70	ACON(39)	$C_{l\delta}$
71-80	ACON(40)	$C_{l\phi}$

CARD NO. 19 (30I1)

1-40	NNCON(1) - NNCON(40)

MANGLE INPUT

CARD NO. 1 (I1)

1	LMN	No. of Rounds

CARD NO. 2a (10A3)

1-30	SHOTN	Title

CARD NO. 3a (8F10.0)

1-10	DPT	Time step
11-20	RHO	Density
21-30	AS	Speed of sound
31-40	AMREF	Reference Mach No.

CARD NO. 4a (8F10.0)

1-10	D1	Reference diameter, inches
11-20	AIX	Axial Moment of Inertia
21-30	AIY	Y-Transverse Moment of Inertia
31-40	AIZ	Z-Transverse Moment of Inertia
41-50	AIXY	Product of Inertia
51-60	WGT	Weight, lbs
61-70	ACG	Offset CG

CARD NO. 5a (8F10.0)

1-10	XCGR	Reference CG, percent of length
11-20	XLR	Reference length, inches
21-30	XCG	CG, percent of length
31-40	XFIN	No. of Fins or Assymetries

88

CARD NO. 6a (8F10.0)

1-10	TCON(1)	θ_{RB_o}, degrees
11-20	TCON(2)	q_o, deg/sec
21-30	TCON(3)	Ψ_{RB_o}, degrees
31-40	TCON(4)	r_o, deg/sec
41-50	TCON(5)	$C_{m\alpha}$ —
51-60	TCON(6)	C_{mq} —
61-70	TCON(7)	$C_{np\alpha}$ —
71-80	TCON(8)	Not used

CARD NO. $7a_{(1)}$ to $7a_{(NT)}$ (8F10.0)

1-10	TIME(K)	Time, sec
11-20	DIST(1,K)	X Distance, ft
21-30	DIST(2,K)	Y Distance, ft
31-40	DIST(3,K)	Z Distance, ft
41-50	PHIX(K)	$\emptyset$, radians
51-60	THETFP(K)	θ_{FP}, degrees
61-70	PSIFP(K)	Ψ_{FP}, degrees

CARD NO. $7a_{(NT+1)}$

1-10	200.	Stop Card

CARD NO. 8a (8F10.0)

1-10	HCON(1)	X_o, feet
11-20	HCON(2)	$\dot{X}_o$, feet/sec
21-30	HCON(3)	Y_o, feet
31-40	HCON(4)	$\dot{Y}_o$, feet/sec

CARD NO. 8a (contd.) (8F10.0)

41-50	HCON(5)	Z_o, feet
51-60	HCON(6)	$\dot{Z}_o$, feet/sec
61-70	HCON(7)	C_{X_o}
71-80	HCON(8)	$C_{X\alpha_2}$

CARD NO. 9a (8F10.0)

1-10	HCON(9)	$C_{X\beta_2}$
11-20	HCON(10)	C_{X_m}
21-30	HCON(11)	C_{Y_o}
31-40	HCON(12)	$C_{Y\beta}$
41-50	HCON(13)	$C_{Y\beta_3}$
51-60	HCON(14)	C_{N_o}
61-70	HCON(15)	$C_{N\alpha}$
71-80	HCON(16)	$C_{N\alpha_3}$

CARD NO. 10a (8F10.0)

1-10	HCON(17)	$C_{Yp\alpha}$
11-20	HCON(18)	$C_{Yp\beta}$
21-30	HCON(19)	$C_{X\bar{\alpha}_2}$
31-40	HCON(20)	$C_{N\bar{\alpha}}$
41-50	HCON(21)	$C_{N\bar{\alpha}_3}$
51-60	HCON(22)	$C_{Yp\bar{\alpha}}$
61-70	HCON(23)	Not Used
71-80	HCON(24)	P_o, rad/sec

90

MANGLE INPUT (continued)

CARD NO. 11a (8F10.0)

1-10	HCON(25)	ϕ_o, radians
11-20	HCON(26)	C_{lp}
21-30	HCON(27)	$C_{l\delta}$
31-40	HCON(28)	$C_{l\phi}$
41-50	HCON(29)	SPNFORM (on $\dfrac{I_y - I_z}{I_x}$)
51-60	HCON(30)	Not used

CARD NO. 12a (30I1)

1-30	NHCON(1) – NHCON(30)

CARD NO. 13a$_{(1)}$ to 13a$_{(NT)}$ (8F10.0)

1-10	TIME(K)	Time, sec
11-20	VEL(K)	Total Velocity, ft/sec
21-30	AQBAR(K)	Dynamic Pressure
31-40	TRB(K)	θ_{RB}, degrees
41-50	PRB(K)	Ψ_{RB}, degrees

CARD NO. 13a$_{(NT+1)}$

1-10	200.	Stop Card

CARD NO. 14a (8F10.0)

1-10	ACON(1)	θ_{RB_o}, degrees
11-20	ACON(2)	q_o, deg/sec
21-30	ACON(3)	Ψ_{RB_o}, degrees
31-40	ACON(4)	r_o, deg/sec

CARD NO. 14a (cont.) (8F10.0)

41-50	ACON(5)	C_{mo}
51-60	ACON(6)	$C_{m\alpha}$
61-70	ACON(7)	$C_{m\alpha_3}$
71-80	ACON(8)	C_{no}

CARD NO. 15a (8F10.0)

1-10	ACON(9)	$C_{n\beta}$
11-20	ACON(10)	$C_{n\beta_3}$
21-30	ACON(11)	C_{mq}
31-40	ACON(12)	C_{mq_2}
41-50	ACON(13)	C_{nr}
51-60	ACON(14)	C_{nr_2}
61-70	ACON(15)	$C_{np\alpha}$
71-80	ACON(16)	$C_{mp\beta}$

CARD NO. 16a (8F10.0)

1-10	ACON(17)	$C_{n\emptyset\bar{\alpha}}$
11-20	ACON(18)	AIXY
21-30	ACON(19)	AIX
31-40	ACON(20)	$C_{m\emptyset\bar{\alpha}}$
41-50	ACON(21)	$C_{m\alpha_2}$
51-60	ACON(22)	$C_{n\alpha_2}$
61-70	ACON(23)	$C_{mo\emptyset}$
71-80	ACON(24)	$C_{mo\emptyset}$

92

MANGLE INPUT <u>(concluded)</u>

CARD NO. 17a (8F10.0)

1-10	ACON(25)	Not used
11-20	ACON(26)	$C_{m\bar{\alpha}}$
21-30	ACON(27)	$C_{m\bar{\alpha}_3}$
31-40	ACON(28)	$C_{m\bar{q}}$
41-50	ACON(29)	$C_{m\bar{q}_2}$
51-60	ACON(30)	$C_{np\bar{\alpha}}$
61-70	ACON(31)	Not used
71-80	ACON(32)	Not used

CARD NO. 18a (8F10.0)

1-10	ACON(33)	Not used
11-20	ACON(34)	Not used
21-30	ACON(35)	Not used
31-40	ACON(36)	ϕ_o, radians
41-50	ACON(37)	p_o, rad/sec
51-60	ACON(38)	C_{1p}
61-70	ACON(39)	$C_{1\delta}$
71-80	ACON(40)	$C_{1\phi}$

CARD NO. 19a (40I1)

1-40	NNCON(LM,1) - NNCON(LM,40)

o   Cards 2 through 19 must be read 'LMN' times, stacked behind each other
    (i.e. 2a-19a, 2b-19b, ...).

o   Cards 8-12 are read to get the HCONS to be used by MANGLE.

o   Cards 14-19 are next to supply the common coefficients for the multiple
    fit and also the unique coefficients (ACON's 1, 2, 3, 4, 5, 8, 18, 19, 36,
    37) of the first data set.

o   Cards 20-22 (Below) are repeated for the remaining data sets to supply the
    unique coefficients for those rounds.

<u>CARD NO. 20 (8F10.0)</u>

1-10	ACON(1)	θ_{RB_o}, degrees
11-20	ACON(2)	q_o, deg/sec
21-30	ACON(3)	Ψ_{RB_o}, degrees
31-40	ACON(4)	r_o, deg/sec
41-50	ACON(5)	C_{mo}
51-60	ACON(8)	C_{no}
61-70	ACON(18)	AIXY
71-80	ACON(19)	AIX

<u>CARD NO. 21 (8F10.0)</u>

1-10	ACON(36)	ϕ_o, radians
11-20	ACON(37)	p_o, rad/sec

<u>CARD NO. 22 (1011)</u>

1-10   NNCON(LM,1) - NNCON(LM,40)

EXAMPLE DATA DECK SETUP

TWO ROUNDS

Card 1 (LMN = 2)

Cards 2a-19a
                            Written by ROLL-HEAVE
Cards 2b-19b

Cards 8-12   HCONS for MANGLE

Cards 14-19
                            ACONS for MANGLE
Cards 20-22

THREE ROUNDS

Card 1 (LMN = 3)

Cards 2a-19a

Cards 2b-19b   Written by ROLL-HEAVE

Cards 2c-19c   :

Cards 8-12   HCONS for MANGLE

Cards 14-19

Cards 20-22   ACONS for MANGLE

Cards 20-22

MUL-HEEV INPUT

IBM Col.

CARD NO. 1 (I1)

1	LMN	Number of Rounds

CARD NO. 2a

1-30	SHOTN	Title

CARD NO. 3a (8F10.0)

1-10	DPT	Time Step
11-20	RHO	Density
21-30	AS	Speed of Sound
31-40	AMREF	Reference Mach No.

CARD NO. 4a (8F10.0)

1-10	D1	Reference diameter, inches
11-20	AIX	Axial Moment of Inertia, lb-in^2
21-30	AIY	Y-Transverse Moment of Inertia, lb-in^2
31-40	AIZ	Z-Transverse Moment of Inertia, lb-in^2
41-50	AIXY	Product of Inertia
51-60	WGT	Weight, lbs
61-70	ACG	Offset, CG

CARD NO. 5a (8F10.0)

1-10	XCGR	Reference CG, percent of length
11-20	XLR	Reference length, inches
21-30	XCG	CG, percent of length
31-40	XFIN	No. of Fins or Assymetries

CARD NO. 6a (8F10.0)

1-10	TCON(1)	θ_{RB_o}, degrees
11-20	TCON(2)	q_o, deg/sec
21-30	TCON(3)	Ψ_{RB_o}, degrees
31-40	TCON(4)	r_o, deg/sec
41-50	TCON(5)	$C_{m\alpha}$
51-60	TCON(6)	C_{mq}
61-70	TCON(7)	$C_{np\alpha}$
71-80	TCON(8)	Not used

CARD NO. 7a$_{(1)}$ to 7a$_{(NT)}$ (8F10.0)   Experimental Data

1-10	TIME(K)	Time, sec
11-20	DIST(1,K)	X Distance, ft
21-30	DIST(2,K)	Y Distance, ft
31-40	DIST(3,K)	Z Distance, ft
41-50	PHIX(K)	$\emptyset$, radians
51-60	THETFP(K)	θ_{FP}, degrees
61-70	PSIFP(K)	Ψ_{FP}, degrees

CARD NO. 7a$_{(NT+1)}$

1-10	200.	Stop Card

CARD NO. 8a$_{(K)}$ to 8a$_{(NNH)}$ (8F10.0)   From ROLL-NUT

1-10	XTIME(K)	Time, sec
11-20	XQ(K)	Q, deg/ft

CARD NO. $8a_{(K)}$ to $8a_{(NNN)}$ (8F10.0)   (continued)

21-30	XR(K)	R, deg/ft
31-40	TRB	θ_{RB}, degrees
41-50	PRB	Ψ_{RB}, degrees
51-60	XPHI(K)	$\emptyset_C$, radians

CARD NO. $8a_{(NNN+1)}$

1-10	200.	Stop Card

CARD NO. 9a (8F10.0)

1-10	ACON(1)	X_o, feet
11-20	ACON(2)	$\dot{X}_o$, ft/sec
21-30	ACON(3)	Y_o, feet
31-40	ACON(4)	$\dot{Y}_o$, ft/sec
41-50	ACON(5)	Z_o, feet
51-60	ACON(6)	$\dot{Z}_o$, ft/sec
61-70	ACON(7)	C_{X_o}
71-80	ACON(8)	$C_{X\alpha_2}$

CARD NO. 10a (8F10.0)

1-10	ACON(9)	$C_{X\beta_2}$
11-20	ACON(10)	C_{X_m}
21-30	ACON(11)	C_{Y_o}
31-40	ACON(12)	$C_{Y\beta}$
41-50	ACON(13)	$C_{Y\beta_3}$
51-60	ACON(14)	C_{N_o}
61-70	ACON(15)	$C_{N\alpha}$
71-80	ACON(16)	$C_{N\alpha_3}$

CARD NO. 11a (8F10.0)

1-10	ACON(17)	$C_{Yp\alpha}$
11-20	ACON(18)	$C_{Yp\beta}$
21-30	ACON(19)	$C_{X\bar{\alpha}_2}$
31-40	ACON(20)	$C_{N\bar{\alpha}}$
41-50	ACON(21)	$C_{N\bar{\alpha}_3}$
51-60	ACON(22)	$C_{Yp\bar{\alpha}}$
61-70	ACON(23)	Not Used
71-80	ACON(24)	P_o, rad/sec

CARD NO. 12a (8F10.0)

1-10	ACON(25)	ϕ_o, radians
11-20	ACON(26)	C_{1p}
21-30	ACON(27)	$C_{1\delta}$
31-40	ACON(28)	$C_{1\phi}$
41-50	ACON(29)	SPNFORM (on $\dfrac{I_y - I_z}{I_x}$)
51-60	ACON(30)	Not used

CARD NO. 13a (30I1)

1-30	NNCON(LM,1) - NNCON(LM,30)

o   Cards 2 through 13 must be read 'LMN' times stacked behind each other
     (i.e., 2a-13a, 2b-13b, ...).

o   Cards 9 through 13 are then read once again containing the initial estimates
     for the common aerodynamics and for the unique coefficients (ACON(1), (2),
     (3), (4), (5), (6), (11), (14), (24), (25), (29)) pertaining to the first
     data set.

o   Cards 14a, 15a, 16a are read for the unique coefficients and NNCON's for the remaining data sets.

CARD NO. 14a (8F10.0)

1-10	ACON(1)	X_o, feet
11-20	ACON(2)	$\dot{X}_o$, ft/sec
21-30	ACON(3)	Y_o, feet
31-40	ACON(4)	$\dot{Y}_o$, ft/sec
41-50	ACON(5)	Z_o, feet
51-60	ACON(6)	$\dot{Z}_o$, ft/sec
61-70	ACON(11)	C_{Y_o}
71-80	ACON(14)	C_{N_o}

CARD NO. 15a (8F10.0)

1-10	ACON(24)	P_o, rad/sec
11-20	ACON(25)	$\emptyset_o$, radians
21-30	ACON(29)	SPNFORM (on $\dfrac{I_y - I_z}{I_x}$)

CARD NO. 16a (11I1)

| 1-11 | | NNCON(LM,1) - NNCON(LM,30) |

MUL-HEEV INPUT (Concluded)

EXAMPLE OF DATA DECK SETUPS

TWO ROUNDS

    Card No. 1   LMN = 2

    Card No. 2a-13a
                              Written by ROLANGLE
    Card No. 2b-13b

    Card No. 9a-13a
                              Coefficient for MUL-HEEV
    Card No. 14a-16a

THREE ROUNDS

    Card No. 1   LMN = 3

    Card No. 2a-13a

    Card No. 2b-13b   Written by ROLANGLE

    Card No. 2c-13c

    Card No. 9a-13a

    Card No. 14a-16a

    Card No. 14b-16b

LIST OF SYMBOLS

i_e, j_e, k_e	—	unit vectors aligned with the earth coordinate system
i_{mf}, j_{mf}, k_{mf}	—	unit vectors aligned with the fixed plane coordinate system
i_m, j_m, k_m	—	unit vectors aligned with the body fixed coordinate system
$\dfrac{d_m}{dt}$	—	derivative with respect to time in body fixed coordinates
m	—	mass of the missile
$\vec{V}$	—	total velocity vector relative to earth
$\vec{\omega}_T$	—	total angular velocity relative to earth
$\vec{J}$	—	total angular momentum of the missile
u_{RB}, v_{RB}, w_{RB}	—	body fixed velocity components relative to earth
p, q, r	—	body fixed angular velocity components relative to earth
I_x	—	mass moment of inertia about the x-axis
I_y	—	mass moment of inertia about the y-axis
I_z	—	mass moment of inertia about the z-axis
I_{xy}	—	cross product of mass moment of inertia
$\dot{u}$	—	indicates the derivative of u with respect to time
$\vec{F}$	—	body fixed total force vector
$\vec{L}$	—	body fixed total moment vector

F_x, F_y, F_z	—	body fixed force components
L_p, L_q, L_r	—	body fixed moment components
θ_{FP}, ψ_{FP}	—	fixed plane Euler angles
ϕ	—	roll angle about the body axis
u_m, v_m, w_m	—	missile fixed velocity components relative to the trajectory
$\bar{q}$	—	dynamic pressure
A	—	reference area of the body
d	—	reference diameter of the body
ϕ'	—	aerodynamic roll angle
t	—	time
ρ	—	air density
θ_{RB}, ψ_{RB}	—	body fixed Euler angles
V_x, V_y, V_z	—	Earth fixed velocity components

INITIAL DISTRIBUTION

Hq USAF/RDQRM	1	Naval Weapons Center/Code 3123	1
Hq USAF/SAMI	1	Ogden ALC/MMWM	2
Hq USAF/XOXFCM	1	AF Spec Comm Cntr/SUR	3
AFSC/IGFG	1	DAMA-WSA	1
AFSC/SDZA	1	SARPA-FR-S-A	1
Hq AFSC/DLCAW	1	US Atomic Energy Comm/Hq Lib	1
AFML/DO/AMIC	1	AEDC/ARO, Inc/DLCS	1
Hq 4950 TW/TZHM	1	AMXSY/DS	1
AFIT/LD	1	AMCRD/WM	1
ASD/ENYS	1	Nav Wpns Eval Fac/Code WT	1
ASD/ENAZ	1	Office of the Chief of Nav Opns/	1
AFFDL/FES	1	(OP-982E)	
TAC/DRA	1	Naval Research Lab/Code 2627	1
SAC/LGWC	1	Hq PACAF/LGWSE	4
Hq SAC/NRI, STINFO Lib	1	USAFTAWC/TE	1
WRAMA/MMEBL	1	TAWC/TRADOCLO	1
CRE/ADD/Publications	2	AFATL/DL	1
AFWL/LR	1	AFATL/DLY	1
AUL (ALU/LSE-70-239)	1	AFATL/DLOU	1
SAPRI-LW-A	1	AFATL/DLOSL	9
AMXSY-DD	1	AFATL/DLYV	1
AMXSY-A	1	AFATL/DLDL	1
DRXBR-TE	1	AFATL/DLDA	1
Lib, K2400	1	AFATL/DLDE	1
SARPA-TS-TS	1	AFATL/DLDT	1
Dahlgren Laboratory	1	AFATL/DLDG	1
White Oak Laboratory	2	AFIS/INTA	1
NAV ORD STN/Tech Lib	1	Naval Sea Systems Comd/Code SEA-	1
NAV WEAPONS STN/20323	1	0332)	
NAV Underwater Systems Ctr/Code 54	1	Naval Sea Systems Comd/Code SEA-	1
USN WEA CNTR/Code 233	2	992E)	
Naval Weapons Center/Code 31	1	Nav Ord Lab/White Oak	2
Air Force Wpns Lab/Tech Lib	1	Naval Wpns Center/Code 32602	1
NAV AIR SYS COMD/Code AIR-532	1	Naval Wpns Center/Code 3163	1
Office Naval Research/Code 473	1	Ogden ALC/MMWRA	2
NASA STINFO FAC	1	AFLC/MMWMC	1
Lawrence Rad Lab/Dept L-3	1	ASD/ENESS	1
The John Hopkins Univ/	1	AFATL/DLJ	2
Applied Physics Lab		AFATL/DLA	1
Battelle Memorial Inst/Reports Lib	1	ADTC/SDC	1
Inst for Defense Analysis/	1	Redstone Sci Info Cntr/Doc Sec	1
Classified Lib		General Electric Co/Armament Dept	10
Sandia Laboratories	2		
The RAND Corp/Lib-D	1		
DDC/TC	2		
USAFTFWC/TA	1		
SARWV-RDT-L	1		